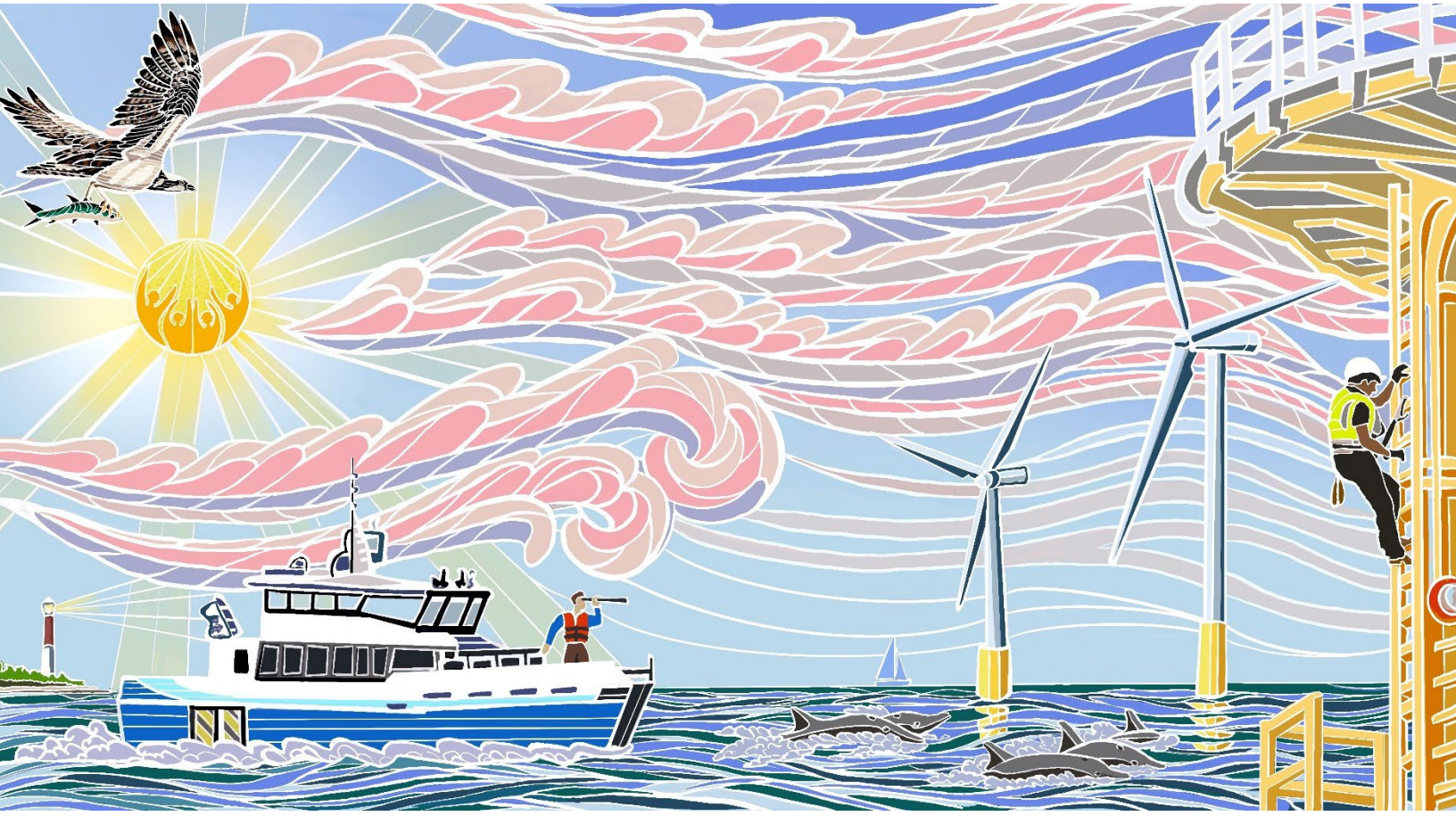

Appendix II-W

Hydraulic Zone of Influence and Offshore Substation Effluent Modeling Report

March 2024

OFFSHORE SUBSTATION EFFLUENT DISCHARGE MODELING AND HYDRAULIC ZONE OF INFLUENCE INTAKE CALCULATIONS

Atlantic Shores North Offshore Project Area

Prepared by:

RPS

Melissa Gloekler, Paxton Albert, Emily Day, Mahmud Monim, Tayebeh Tajalli Bakhsh, and Jill Rowe

55 Village Square Drive
South Kingstown, RI 02879

T 401-661-8656

E Missy.Gloekler@rpsgroup.com

Prepared for:

EDR

22-P-210815

ASOW North
V1

March 30, 2023

EXECUTIVE SUMMARY

Study Summary and Goals

Atlantic Shores Offshore Wind, LLC (Atlantic Shores), a 50/50 joint venture between EDF-RE Offshore Development, LLC, a wholly owned subsidiary of EDF Renewables, Inc. (EDF Renewables) and Shell New Energies US LLC (Shell), is proposing to develop an offshore wind energy generation project within the Lease Area OCS-A 0549 (herein referred to as the Lease Area). The Lease Area is approximately 81,129 acres (328.3 km^2) in size and is located on the Outer Continental Shelf (OCS) within the New Jersey Wind Energy Area (WEA). The New Jersey WEA was identified as suitable for offshore renewable energy development by the Bureau of Ocean Energy Management (BOEM) through a multi-year, public environmental review process. At its closest point, the Lease Area is approximately 8.4 miles (mi) (13.5 kilometers [km]) from the New Jersey State coast and approximately 60 mi (96.6 km) from the New York State coast. The facilities to be installed within the Lease Area will include a maximum of up to 157 wind turbine generators (WTGs) and up to 8 small, 4 medium, or 3 large offshore substations (OSSs).

Transmitting the renewable energy generated in an offshore wind farm to an onshore POI for injection into the onshore grid requires that the transmission voltage is increased at the offshore substation. Depending on the distance to shore, grid interconnection requirements, and many other potential drivers, there may be an additional need to convert the high voltage alternating current (HVAC) to high voltage direct current (HVDC) at the OSS. Heat is generated in the HVAC voltage transformation process, and if HVAC to HVDC conversion is required, additional heat is generated as a by-product of this conversion. As a result, these sensitive high voltage systems must be continuously cooled when in operation, with a greater cooling demand required for an HVDC OSS compared with a traditional HVAC OSS. To provide the additional cooling capacity required for an HVDC OSS, seawater is used to absorb and reject the excess heat. This cooling seawater would be brought onto the OSS via a subsurface intake, pumped through a heat exchanger to absorb the excess equipment heat, and discharged back into the environment with a subsurface discharge at an elevated temperature. Additionally, the seawater may be filtered to remove small particulates and treated to prevent biofouling of the cooling system equipment.

RPS performed a water quality assessment to investigate the hydraulic zone of influence (HZI) created during water intake operations, and using the USEPA-approved CORMIX model, computational effluent discharge modeling was conducted to predict the magnitude, and extent of the effluent plumes above background values and in association with the potential dilution that would result. From these analyses, the dilution of the thermal plume and residual chlorine concentrations from a representative OSS location were predicted. The results provided in this assessment are representative of the types of releases that would be anticipated from an HVDC OSS cooling water system and are therefore useful in determining the scale and magnitude of potential effects.

These studies accounted for seasonality, the influence of ambient current velocities, and variable flow rates from two, 2100 MW and 1400 MW, potential OSS cooling water systems. To bound the potential environmental and design conditions associated with the OSSs, 24 effluent discharge configurations were evaluated using design configurations associated with a 2100 MW and 1400 MW HVDC systems. To be conservative, the largest temperature differential was evaluated for both the 1400 MW and 2100 MW HVDC's, while the influence of flow rate was evaluated using the 2100 MW HVDC as an upper bound and the 1400 MW HVDC as a lower bound.

Environmental Conditions

To predict the behavior of the HZI and effluent discharges, it is necessary to understand the predominant environmental conditions within the area of interest. The HZI calculations are highly dependent on the ambient current speeds at the intake location. Winds, currents, and the physical characteristics of water

column (including temperature, salinity, and density) are the key parameters that influence transport, physical fate, and ultimately the dilution of discharges in receiving waters. To simulate environmental conditions, wind and current speeds were evaluated over 10 years. Long-term records of wind and current data were obtained from regional atmospheric and ocean circulation models for this study, and water column characteristics (e.g., temperature, salinity, density) were obtained from high resolution records from the World Ocean Atlas (2018) climatological data set.

Seasonality was accounted for by applying depth dependent minimum temperatures within the water column for spring, summer, fall, and winter. Monthly average wind speeds range from 5 to 8 m/s with the strongest average winds occurring in the winter (~ 8 m/s) and the weakest average wind in summer (~5 m/s). For the HZI calculations, the 5th- and 95th-percentile current speeds were depth-averaged to bound the minimum and maximum current speeds that could be observed at the intake locations. The depth-averaged 5th-percentile current speed used was 0.02 m/s and the 95th-percentile current speed used was 0.34 m/s. To capture the influence of wind on plume dispersion, a value of 6.5 m/s was applied in the CORMIX OSS effluent discharge modeling. Velocity profiles capturing the 5th-, 50th-, and 95th-percentile current speeds were calculated over the entire 10-year dataset and were used to evaluate the influence of ambient current speeds on the plume dynamics for each season. These ambient current speeds at the discharge depth ranged from 0.02 m/s to 0.29 m/s.

Results and Conclusions

The HZI calculations were performed assuming the maximum and minimum operational intake rates, as well as the 5th- and 95th-percentile current speeds. This allowed the results to be bounded between the highest and lowest expected HZI value expected at the large OSS site. When modeling the various effluent types, it was assumed that the constituents of interest present were conservative (i.e., non-reactive, non-degrading), the environmental conditions were at steady state (i.e., do not change with time), and background concentrations of the constituents were negligible. Therefore, results from the simulations represent a snapshot in time and may change at the time of the release based on spatially- and temporally varying parameters (e.g., currents, winds) or the exact discharge conditions (e.g., flow rate, pipe diameter, discharge depth).

Under all conditions, the maximum HZI is predicted to be 0.116 m from the intake location and the minimum HZI is predicted to be 0.001 m from the intake location. In general, predictions showed that as the intake velocities increase and the ambient current speeds decrease, a larger HZI will form. Conversely, with higher current speeds and lower intake velocities, the HZI will decrease in size. It should be noted that with evolving current speeds and operational intake rates, the HZI will change at the large OSS location (Table ES-0-1).

Table ES-0-1: Summary of calculated HZI results.

HZI	Minimum Operational Flow (5th-Percentile Currents)	Minimum Operational Flow (95th-Percentile Currents)	Maximum Operational Flow (5th-Percentile Currents)	Maximum Operational Flow (95th-Percentile Currents)
R_{HZI} (m)	0.023	0.001	0.116	0.007
R_{HZI} (ft)	0.076	0.004	0.381	0.022

For the thermal plume discharges, plume dynamics and dilution factors were primarily impacted by the total volume of the release, seasonality of the release, and the associated current speeds (Table ES-0-2). Overall, all simulated cases met the water quality standards (WQS') for both the excess temperature threshold of 3°C temperature excess and 0.5 mg/L of residual chlorine. These WQS' generally were met within 10 m of the discharge point, but two simulated cases reached up to 32 m from the discharge point before dropping below the thresholds.

As each simulated plume was discharged into the ambient environment, the thermal plumes experienced rapid mixing and were sufficiently diluted as they traveled downstream from the discharge point. Higher rates of discharge predicted faster mixing in close proximity (<1 m) with the discharge pipe, which was observed with the 2100 MW HVDC scenarios. Contrarily, the 1400 MW HVDC scenarios showed similar, but slightly less mixing within the same <1 m distance. Seasonality differences were observed in the plume simulations, mostly due to stratification effects within the water column, where the most stratified season (summer) showed the lowest potential for mixing. The least stratified environment (winter) predicted the most potential for mixing in general. Current speeds also affected the plume dynamics. In general, higher current speeds exhibited the plume traveling further downstream before meeting the WQS', but also predicted the smallest lateral plume radius at 100 m from the discharge point. In summary, the plume behavior and dilution are highly dependent on the environmental conditions present at the discharge location and the operational conditions that initialize the discharged plume. However, based on the model input parameters, the predicted dilution would be sufficient to minimize potential water quality impacts outside of 100 m for all scenarios considered.

Table ES-0-2: Summary of plume extent and dilution results.

Season	Water Quality Standard: 3°C Excess Downstream Distance (m)	Water Quality Standard: 0.5 mg/L Chlorine Residual Downstream Distance (m)	Dilution Factor at 100 m Downstream Distance	Lateral Plume Radius (m) at 100 m Downstream Distance
1400 MW Cooling Water Discharge				
Spring 5th percentile	1.39	0.29	49.1	191.19
Spring 50th percentile	4.75	0.60	38.3	33.00
Spring 95th percentile	7.68	0.38	52.8	8.32
Summer 5th percentile	0.96	0.38	20.8	137.62
Summer 50th percentile	3.68	0.61	15.2	32.22
Summer 95th percentile	6.58	0.40	33.2	12.75
Fall 5th percentile	0.84	0.38	80.7	296.46
Fall 50th percentile	3.61	0.60	39.0	40.34
Fall 95th percentile	6.46	0.38	64.3	10.39
Winter 5th percentile	1.23	0.29	55.1	210.81
Winter 50th percentile	4.49	0.59	48.1	34.78
Winter 95th percentile	7.54	0.38	67.6	8.48
2100 MW Cooling Water Discharge				
Spring 5th percentile	1.64	0.12	55.2	264.43
Spring 50th percentile	4.99	0.42	34.2	37.68
Spring 95th percentile	3.63	0.43	49.2	9.42
Summer 5th percentile	1.04	0.17	17.3	158.32
Summer 50th percentile	15.69	5.38	7.1	44.68
Summer 95th percentile	31.94	5.80	7.1	12.76
Fall 5th percentile	1.04	0.18	64.8	379.13
Fall 50th percentile	4.29	0.53	32.6	46.55
Fall 95th percentile	7.05	0.43	57.8	11.74
Winter 5th percentile	1.51	0.13	58.8	291.60
Winter 50th percentile	4.98	0.42	41.6	39.63
Winter 95th percentile	3.81	0.43	61.4	9.58

CONTENTS

Figures

Tables

List of Acronyms

BOEM	Bureau of Ocean Energy Management
CFSR	Climate Forecast System Reanalysis
GPD	Gallons per day
HF	High Frequency
HVDC	High Voltage Direct Current
HYCOM	Hybrid Coordinate Ocean Model
HZI	Hydraulic Zone of Influence
MB	Mid-Atlantic Bight
NAVOCEANO	Naval Oceanographic Office
NCEI	National Centers for Environmental Information
NCEP	National Center for Environmental Prediction
NCODA	Navy Coupled Ocean Data Assimilation
NOAA	National Oceanic and Atmospheric Administration
OCS	Outer Continental Shelf
OSS	Offshore Substation
SST	Sea Surface Temperature
USEPA	United States Environmental Protection Agency
WEA	Wind Energy Area
WOA	World Ocean Atlas
WQS	Water Quality Standard
WTG	Wind Turbine Generator

1 INTRODUCTION

Atlantic Shores Offshore Wind, LLC (Atlantic Shores), a 50/50 joint venture between EDF-RE Offshore Development, LLC, a wholly owned subsidiary of EDF Renewables, Inc. (EDF Renewables) and Shell New Energies US LLC (Shell), is proposing to develop an offshore wind energy generation project within the Lease Area OCS-A 0549 (herein referred to as the Lease Area; Figure 1-1). The Lease Area is approximately 81,129 acres (328.3 km^2) in size and is located on the Outer Continental Shelf (OCS) within the New Jersey Wind Energy Area (WEA). The New Jersey WEA was identified as suitable for offshore renewable energy development by the Bureau of Ocean Energy Management (BOEM) through a multi-year, public environmental review process. At its closest point, the Lease Area is approximately 8.4 miles (mi) (13.5 kilometers [km]) from the New Jersey coast and approximately 60 mi (96.6 km) from the New York State coast. The facilities to be installed within the Lease Area will include a maximum of up to 157 wind turbine generators (WTGs) and up to 8 small, 4 medium, or 3 large offshore substations (OSSs).

Transmitting the renewable energy generated in an offshore wind farm to an onshore POI for injection into the onshore grid requires that the transmission voltage is increased at the offshore substation. Depending on the distance to shore, grid interconnection requirements, and many other potential drivers, there may be an additional need to convert the high voltage alternating current (HVAC) to high voltage direct current (HVDC) at the OSS. Heat is generated in the HVAC voltage transformation process, and if HVAC to HVDC conversion is required, additional heat is generated as a by-product of this conversion. As a result, these sensitive high voltage systems must be continuously cooled when in operation, with a greater cooling demand required for an HVDC OSS compared with a traditional HVAC OSS. To provide the additional cooling capacity required for an HVDC OSS, seawater is used to absorb and reject the excess heat. This cooling seawater would be brought onto the OSS via a subsurface intake, pumped through a heat exchanger to absorb the excess equipment heat, and discharged back into the environment with a subsurface discharge at an elevated temperature. Additionally, the seawater may be filtered to remove small particulates and treated to prevent biofouling of the cooling system equipment.

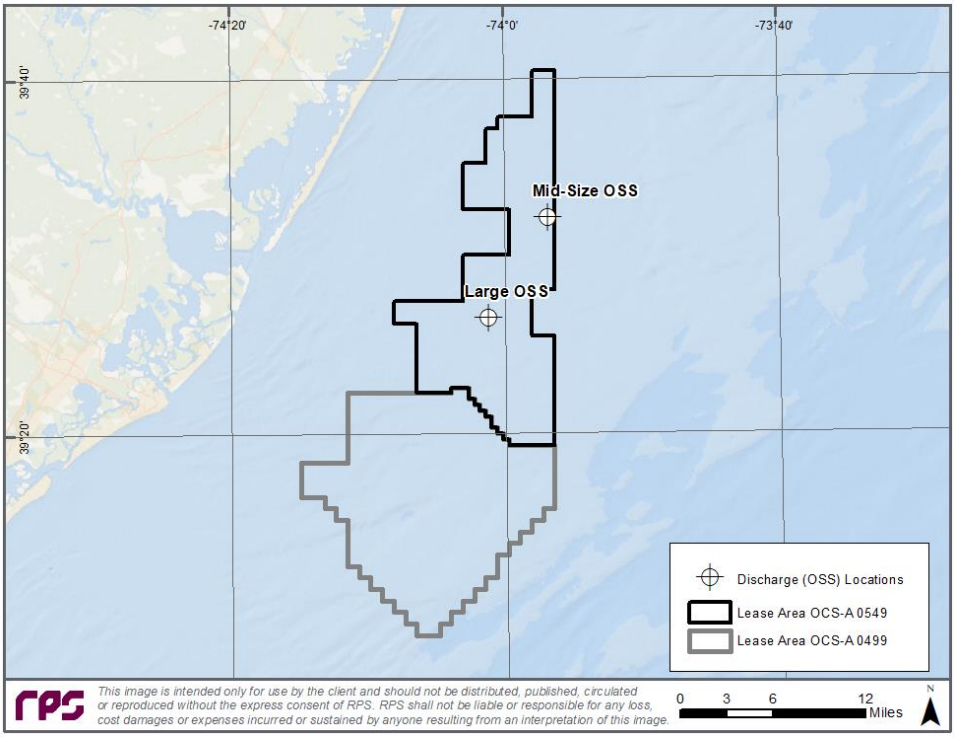

Figure 1-1: Project components and study area.

RPS performed a water quality assessment to investigate the hydraulic zone of influence (HZI) created during water intake operations, and using the USEPA-approved CORMIX model, computational effluent discharge modeling was conducted to predict the magnitude, and extent of the effluent plumes above background values and in association with the potential dilution that would result. From these analyses, the portion of the surrounding water body affected by the withdrawal of the source water and the dilution of the discharged thermal plume and residual chlorine concentrations from a representative large OSS location were predicted. The results provided in this assessment are representative of the intake withdrawal effects and types of releases that would be anticipated from a large OSS cooling water system and are therefore useful in determining the scale and magnitude of potential effects.

These studies accounted for seasonality, the influence of ambient current velocities, and variable flow rates from two, 2100 MW and 1400 MW, potential OSS cooling water systems (Table 1-1). To bound the potential environmental and design conditions associated with the OSSs, 4 HZI calculations were performed. Additionally, 24 effluent discharge configurations were evaluated using design configurations associated with a 2100 MW and 1400 MW systems. To be conservative, the largest temperature differential was evaluated for both the 1400 MW and 2100 MW, while the influence of flow rate was evaluated using the 2100 MW as an upper bound and the 1400 MW as a lower bound.

Table 1-1. Summary of modeled discharge flows.

Modeled Discharge Location	Effluent Type	1400MW (gpd)	2100MW (gpd)	Seasons
Large OSS	Cooling Water	5,880,000	8,820,000	Spring, Summer, Fall, Winter

When modeling the various effluent types, it was assumed that the constituents of interest present were conservative (i.e., non-reactive, non-degrading), the environmental conditions were at steady state (i.e., do not change with time), and background concentrations of the constituents were negligible. Therefore, results from the simulations represent a snapshot in time and may change at the time of the release based on spatially- and temporally varying parameters (e.g., currents, winds) or the exact discharge conditions (e.g., flow rate, pipe diameter, discharge depth).

2 TECHNICAL APPROACH

2.1 HZI Intake Calculations

As part of the planned OSS operations, water will be extracted from the ambient environment and used as cooling water for HVDC systems. The intake of water from these systems creates an HZI. The HZI is the portion of the study area that is hydraulically influenced by the withdrawal of ambient water by the intake system. Beyond the HZI, the ambient currents dominate flow (Golder Associates, 2008). Within the HZI, impingement and entrainment of organisms passing by the cooling water intake structure can occur (Richardson and Dixon, 2004), thus it is important to calculate the extent that it will reach from the intake location. To quantify the HZI at the Atlantic Shores OSS, flow can be estimated from continuity using the following formula (Wiegel, 1964), with additional information available in Richardson and Dixon, 2004 and Golder Associates, 2008:

$$R_{HZI} = Q_i \times \frac{180/\theta}{\pi \times d_r \times V_{ma}}$$

Where R_{HZI} represents the HZI (m), Q_i represents the design intake flow rate (m^3/s), θ represents the angle to the bank (°), d_r is the mean ambient water depth, and V_{ma} is the ambient mean velocity.

2.2 OSS Effluent Discharge Modeling

The OSS effluent discharge modeling was performed using CORMIX, a series of software systems approved by the United States Environmental Protection Agency (USEPA) that was developed for the analysis of aqueous discharges into waterbodies. It has the capability to simulate plumes from submerged single-port (i.e., single-outlet), multi-port, and surface discharges (Doneker and Jirka, 2007). CORMIX contains a rule-based algorithm to classify the flow behavior and implement the appropriate numerical modeling solution based on the release and environmental conditions defined. The model solution predicts the steady state shape, extent, and dilution of an effluent plume from a constant discharge into uniform ambient currents. It considers the interaction of the effluent plume with the boundaries, such as the water surface and the bottom, and allows the formation of subsurface termination (intrusion formation at trap levels) of plumes in density-stratified environments. While CORMIX is not a dynamic model that can reflect time-varying changes in discharge or environmental conditions, it can be used to predict snapshots of the range of anticipated conditions, which can be provided with context representing their statistical significance (e.g., 5th percentile ambient current speed).

CORMIX modeling is used as a standard approach to provide an assessment of expected initial dilution. The model contains both near-field and far-field predictions. The near-field mixing process refers to the region in which the discharge properties dictate the plume characteristics dominated by initial momentum, buoyancy, and geometric orientation of the plume, and the far-field mixing process refers to the region in which the fate and transport of the discharge is dominated by the environmental conditions such as ambient currents. Both the near- and far-field results were simulated but only near-field results and far-field up to 100 m are presented for this study. Far-field results may not be representative in some long duration simulations due to spatial and temporal changes in environmental conditions that take place.

The model provides predictions of the plume position, geometry, and the “dilution factor” as a function of distance and time from the release. The dilution factor, a useful indicator of the fate of discharged constituents in the near-field, is the multiple by which the discharge concentration would be attenuated by mixing with receiving ambient water.

CORMIX simulations require definition of discharge conditions and receiving water characteristics. The modeling inputs required are summarized below:

- Volume flow rate of the discharge and constituent concentration (defines constituent load into the receiving water);
- Discharge pipe diameter used with flow to calculate an exit velocity (determines ability to entrain water, promoting dilution);
- Discharge density (determines if effluent sinks or floats);
- Location and type of discharge (including vertical position: surface, subsurface, or bottom discharge);
- Orientation of the discharge pipe (pointing up or down, opposing or in alignment with the ambient flow direction);
- Ambient currents at the discharge location (affects entrainment and transport); and
- Ambient density of the receiving water.

Using detailed information on the receiving water and initial discharge concentrations, the predicted dilution factors can be used to infer trends of anticipated concentrations within the environment. For this study, a conservative (i.e., non-reacting, non-decaying) constituent was assessed to provide an upper-bound estimate of the magnitude and extent of the discharge as "excess concentrations" (i.e., concentration above background levels) in the receiving waters. Because the targeted constituent was not allowed to react or decay, more would be left in the receiving waters. Therefore, this methodology provided the most conservative estimate of the fate of any discharged constituent of interest.

3 MODEL INPUT DATA

The potential effects of various water discharges were evaluated by the spatial characteristics of the discharge plume and its dilution along the plume centerline for each discharge scenario. The methods for this evaluation included establishing the potential discharges and simulating the discharges within the receiving waters at varying environmental conditions using the dilution model in CORMIX (Doneker and Jirka 1990, 2001, & 2007). The details of the inputs used to simulate the discharge characteristics, the environmental conditions, and the modeling scenario matrix are described in this section.

Cooling water discharges were modeled at a representative large OSS, with the outfall configuration pointing down towards the seabed. Background concentrations of the targeted constituents in the receiving waters were conservatively assumed to be negligible (i.e., zero). Results were evaluated at a distance of 100 m from the discharge locations, which is an extent commonly applied for effluent discharges and is referenced in the United States Code of Federal Regulations (40 CFR 125.121) for terms relevant to Criteria and Standards for the National Pollutant Discharge Elimination System.

3.1 Environmental Conditions

To predict the behavior of effluent discharges, it is necessary to understand the predominant environmental conditions within the area of interest. Winds, currents, and the physical characteristics of water column (including temperature, salinity, and density) are the key parameters that influence transport, physical fate, and ultimately the dilution of discharges in receiving waters. To simulate environmental conditions, wind and current speeds were evaluated over 10 years. Long-term records of wind and current data were obtained from regional atmospheric and ocean circulation models for this study. The following sections describe the predominant environmental conditions relevant to this study.

3.1.1 Regional Dynamics and Climatology

The sites of interest are located within the Mid-Atlantic Bight (MAB) near the coast of New Jersey. The MAB is influenced by a southward flowing cool water current from New England and the northward flowing Gulf Stream that migrates northeast after reaching Cape Hatteras at 35°N. The current pattern near the sites exhibit spatial and temporal variation due to the flow of these opposing currents. In addition to these large-scale currents, there are also small-scale currents that are caused by wave refractions and rip currents. Beardsley and Winant (1979) suggest the flow along the MAB region is driven by river runoff, large scale wind stress, and heat flux. Gong et al. (2010) further distinguishes the driving mechanisms of the surface flow on the New Jersey Shelf as a function of topography, seasonal stratification, and wind forcing. High-frequency (HF) radar data manifest the current along the New Jersey shelf flows southwest, generally following the southward flowing current described above (Kohut et al. 2004; Gong et al. 2010). HF radar data from 2002 to 2007 showed that the mean surface flow is between 2 and 12 cm/s (Gong et al. 2010). During the summer, southwest winds also drive cross-shelf offshore flow through Ekman transport.

Data obtained from the World Ocean Atlas (WOA) climatology dataset (Zweng et al. 2018; Locarnini et al. 2018) for the large OSS show the monthly sea surface water temperature typically varies from 5°C to 23°C

(Figure 3-1:Figure 3-1:). The warmest temperatures occur during the summer season and the coldest temperatures occur in the winter and early spring. The site shows a range of salinity from 30.4 ppt to 32.6 ppt with highs in the winter and a decrease into the summer due to increased freshwater discharge during summer as compared to winter (Richaud et al., 2016).

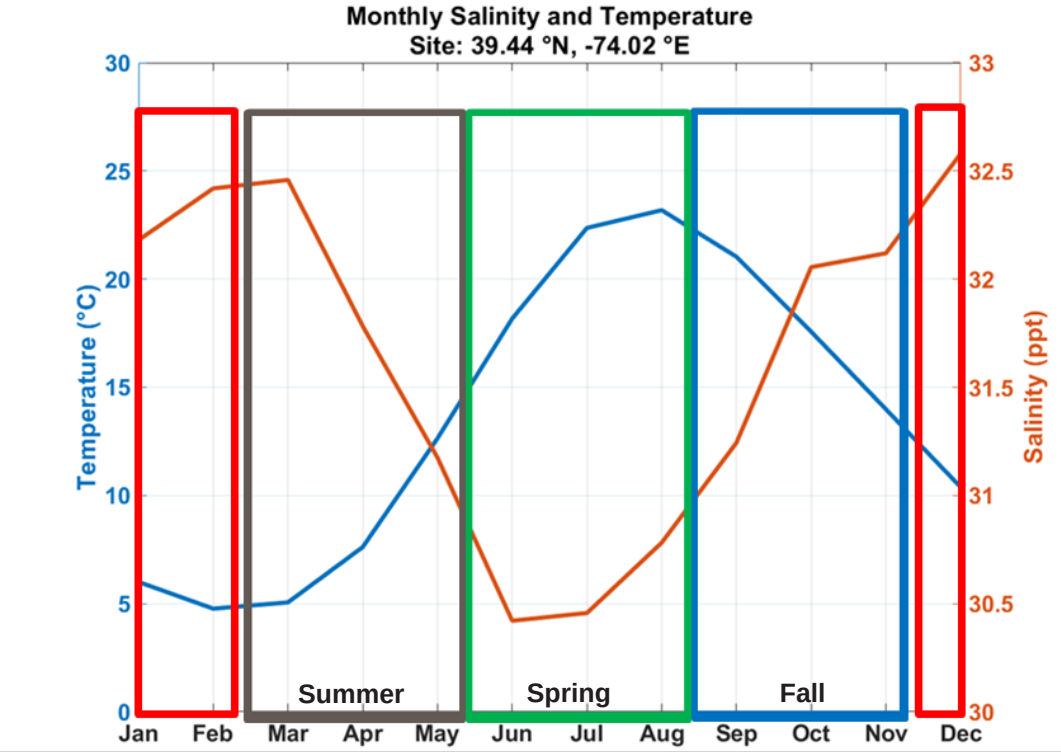

Figure 3-1: Monthly sea surface temperature (°C) in blue and salinity (ppt) in orange near the spill site Large OSS from WOA 2018 (Zweng et al. 2018 and Locarnini et al. 2018). The grey box shows spring, green box shows summer, blue box shows fall, and red boxes show winter.

3.1.2 Winds

For this study, wind data were obtained from the U.S. National Centers for Environmental Prediction (NCEP) Climate Forecast System Reanalysis (CFSR) for a 10-year period (2001 to 2010; Table 3-1). The CFSR model was designed and executed as a global, high-resolution, coupled atmosphere-ocean-land surface-sea ice system to provide the best estimate of the state of these coupled domains (Saha et al., 2010). This atmospheric model has a horizontal resolution of 38 km, with 64 vertical levels extending from the surface to the height at which air pressure reaches 0.26 hPa. CFSR winds were also one of the main driving forces used in the HYCOM (HYbrid Coordinate Ocean Model). Reanalysis, the global hydrodynamic currents dataset used in this study.

Table 3-1: The specifics of wind dataset used for the modeling.

Name of Dataset	CFSR
Coverage	75°W - 69°W 42°N - 39°N
Owner/Provider	NCEP (US)
Horizontal Grid Size	0.5°x0.5°
Hindcast Period	2001 - 2010
Time Step	6 hourly

Wind speeds pertaining to the location of the large OSS are developed using a distance-weighted interpolation from the four surrounding CFSR nodes (Figure 3-2). The area experiences offshore winds predominantly coming from northwest and southwest sector that increase in strength offshore, with a higher percentage of wind speeds found over 8 m/s. The wind direction generally ranges from northwest to south-southwest near the large OSS. The monthly average wind speed ranges from 5 to 8 m/s. The strongest average winds occur in the winter (~ 8 m/s) and the weakest average wind occur in the summer (~5 m/s). To capture the influence of wind on plume dispersion, a value of 6.5 m/s was applied in the CORMIX OSS effluent discharge modeling.

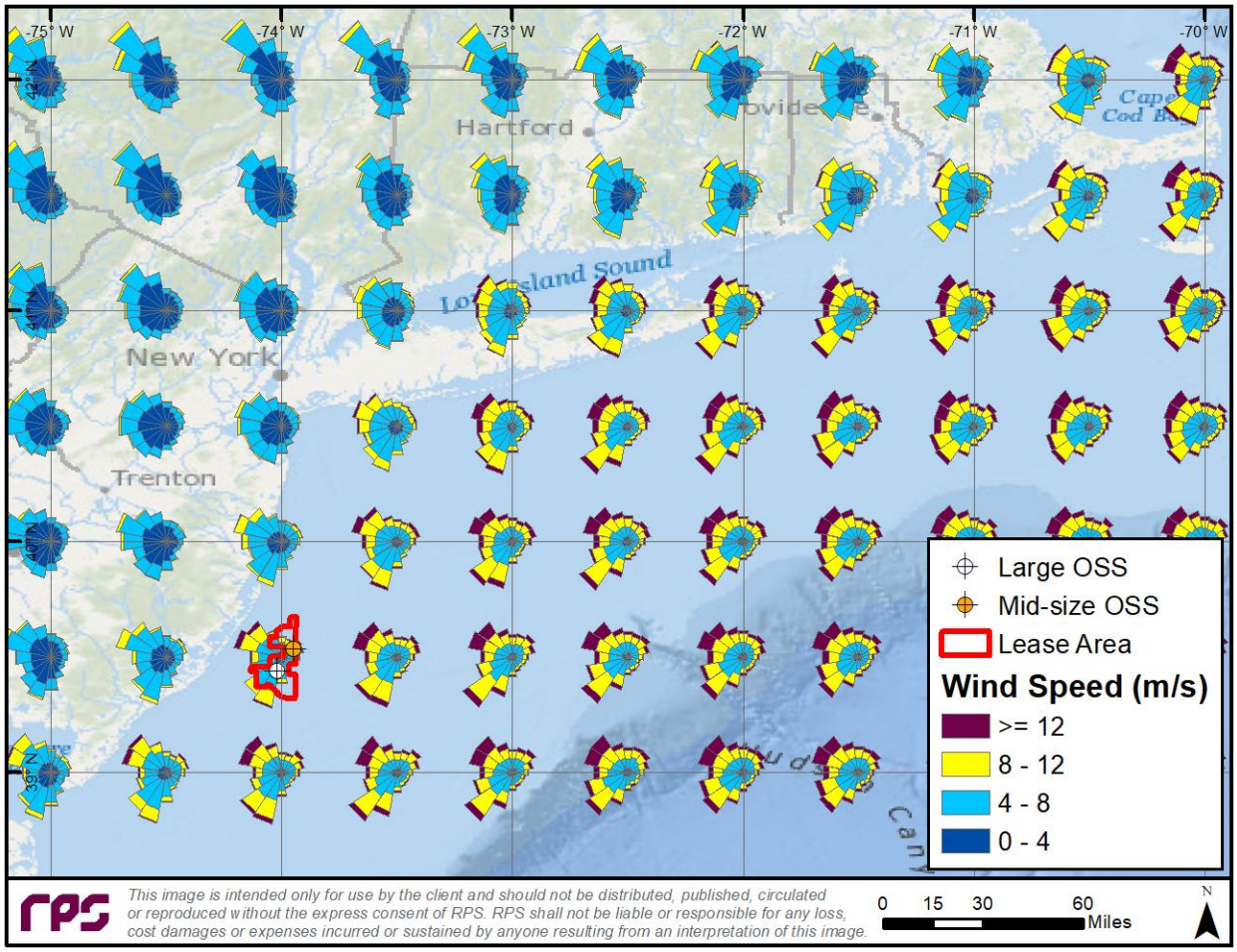

Figure 3-2: Spatial distribution of CFSR annual wind speed and direction used in this study.

3.1.3 Currents

Current data were obtained from the HYCOM hindcast reanalysis, a 1/12-degree global simulation assimilated with NCODA (Navy Coupled Ocean Data Assimilation) from the US Naval Research Laboratory (Halliwell, 2004). This dataset captures the oceanic large-scale circulation in the area of interest (Table 3-2). NCODA uses the model forecast as a first guess in a three-dimensional (3D) variational scheme and assimilates available satellite altimeter observations from the Naval Oceanographic Office (NAVOCEANO) Altimeter Data Fusion Center, *in-situ* Sea Surface Temperature (SST), and available *in-situ* vertical temperature and salinity profiles from XBTs (Expendable Bathythermographs), Argo floats, and moored buoys. Details of the data assimilation procedure are described in Cummings and Smedstad (2013) and Cummings (2005). Fox et al. (2002) describes the technique for projecting surface information (collected for assimilation) downward. Forcing for the model come from the US National Centers for Environmental

Prediction (NCEP) CFSR (Saha et al., 2010). Ocean dynamics including geostrophic, and wind driven currents are reproduced by the model. The most recent reanalysis experiment (GLBu0.08/expt_19.1) includes data between August 1, 1995 and December 31, 2012.

Table 3-2. The specifics of the current datasets used for the modeling.

Dataset	HYCOM (GLBu0.08/expt_19.1)
Owner/Provider	Naval Research Laboratory (USA)
Bathymetry	GEBCO
Wind Forcing	CFSR (US)
Tides	-
Horizontal Grid Size	1/12 degree (~9 km)
Hindcast Period	2001 - 2010
Output Frequency	Daily

Currents extracted from the location of the large OSS show current flow primarily in the northeast/east-northeast, and southwest directions. During the winter, the surface current direction ranges from northeast to southwest via southeast. In summer, the current direction is primarily in the northeast and east-northeast directions. In spring and fall, the current flows are stronger and in the northeast and southwest directions. The 5th-, 50th-, and 95th-percentile current speeds for the area were determined over the 10 year hindcast period (2001 -2010). Variation between surface and bottom currents are greatest under the 95th-percentile (Figure 3-3).

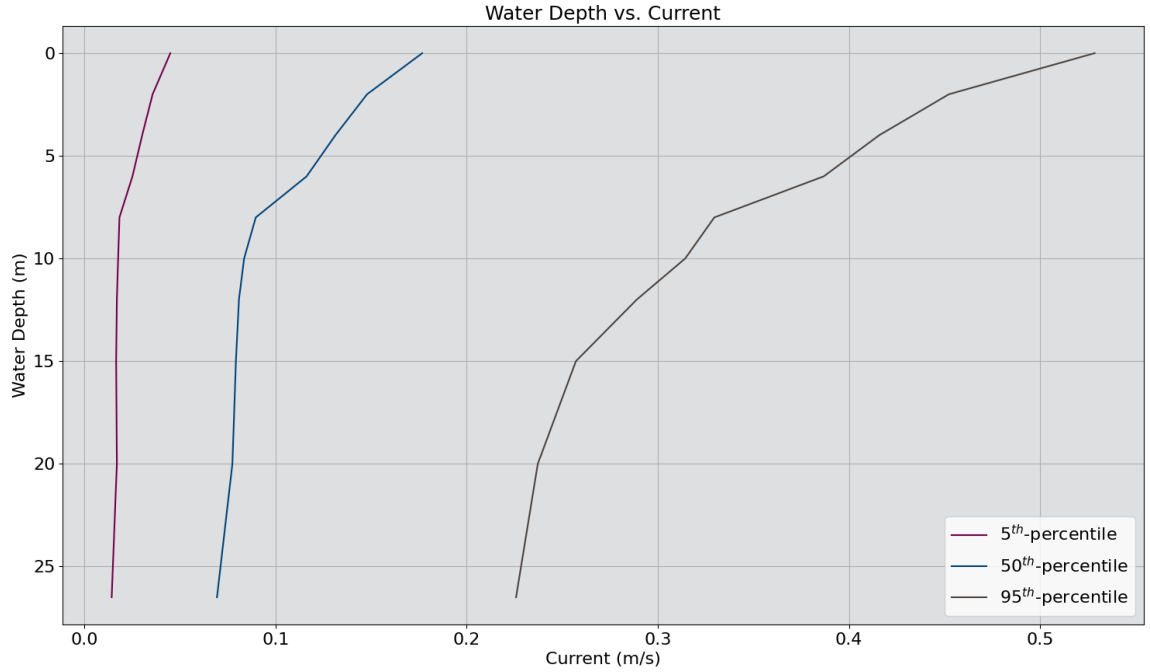

Figure 3-3: Horizontal current speeds (cm/s) from HYCOM. The variation of current speed with depth is provided for 5th-percentile, 50th-percentile, and 95th-percentile.

3.1.4 Temperature, Salinity, and Density

Temperature and salinity were obtained from the WOA 2018 (Zweng et al., 2018; Locarnini et al., 2018) high-resolution dataset, which is distributed online by National Centers for Environmental Information (NCEI). The WOA originated from the Climatological Atlas of the World Ocean and was updated with new data records in 1994, 1998, 2001, 2013, and 2018 (Levitus, 1982; Conkright et al., 2002; Levitus et al., 2013). The WOA 18 includes analyses on a quarter-degree grid for temperature and salinity. The ocean variable analyses are produced on 102 depth levels from the surface to 5,500 m depth.

For this study, temperature (Figure 3-4) and salinity (Figure 3-5) data were extracted at the four grid points closest to the project location and interpolated to estimate the average value at the large OSS. Temperature and salinity values were used in the CORMIX OSS effluent discharge modeling study to estimate the density profile (Figure 3-6).

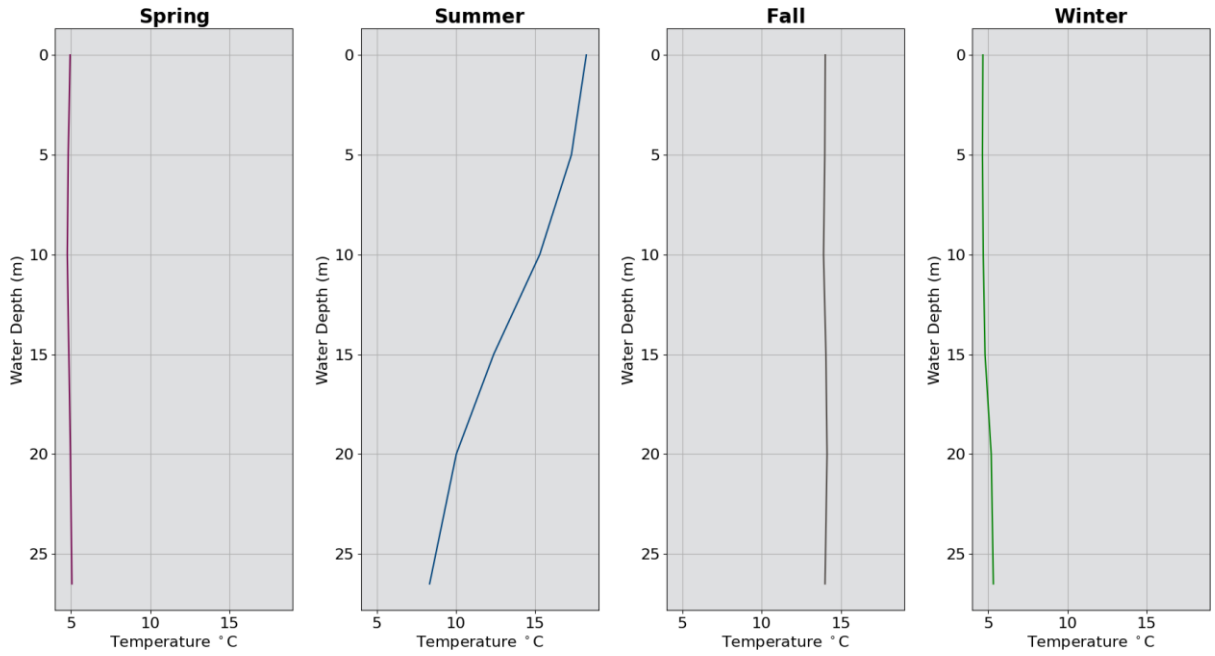

Figure 3-4: Vertical temperature profiles for spring, summer, fall, and winter.

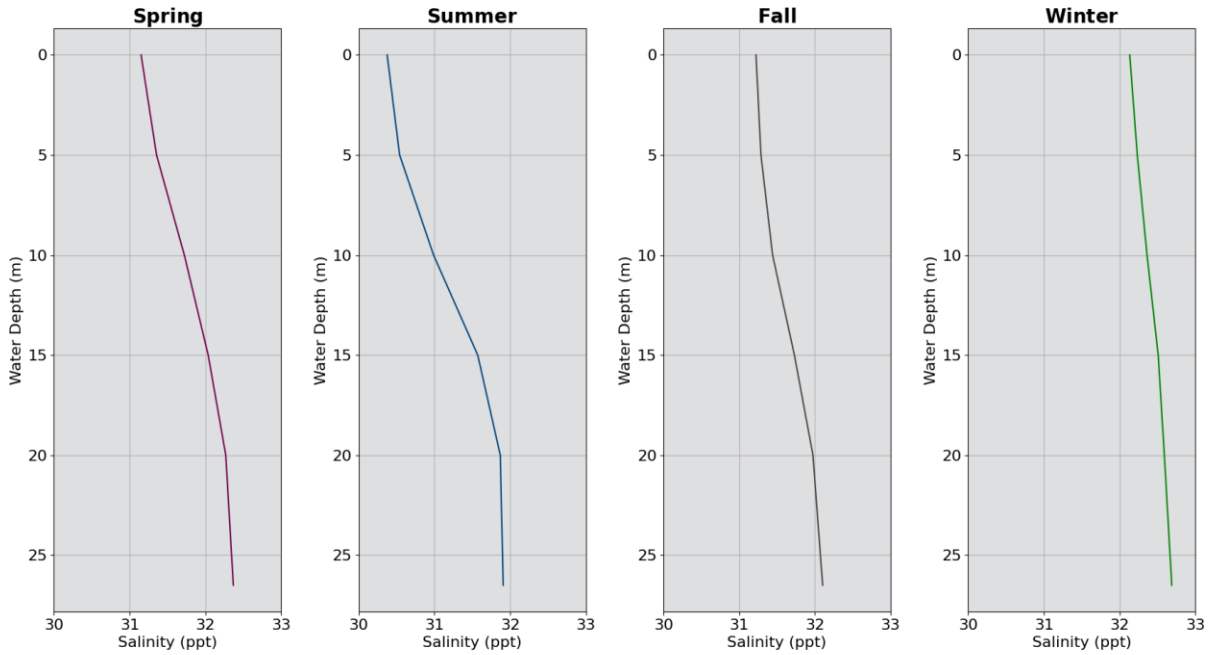

Figure 3-5: Vertical salinity profiles for spring, summer, fall, and winter.

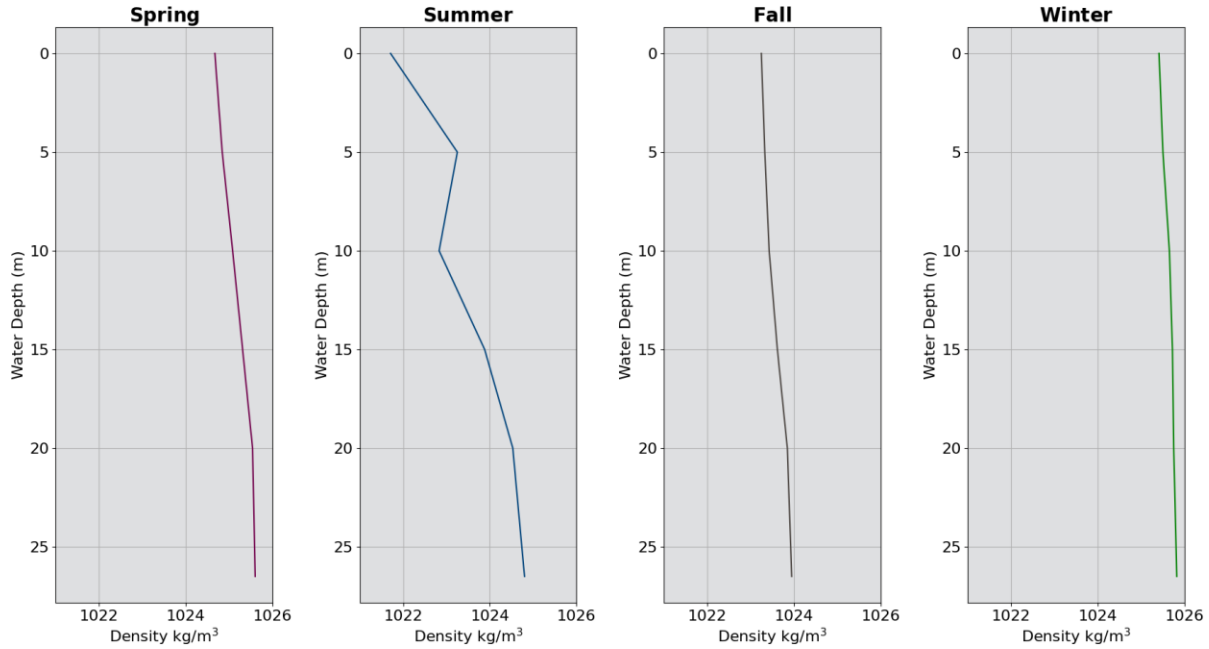

Figure 3-6: Vertical density profiles for spring, summer, fall, and winter.

3.2 HZI Intake Calculations

For this study, a strategy was formulated to bound the lower and upper estimates of the HZI's caused by intake of seawater. The HZI's were calculated using the expected maximum and minimum operational intake flow rates during both the 5th- and 95th-percentile current speeds exhibited in the study area (Table 3-3).

Table 3-3: Inputs for the HZI calculations at the Atlantic Shores OSS.

Parameter	Minimum Operational Flow (5th-Percentile Currents)	Minimum Operational Flow (95th-Percentile Currents)	Maximum Operational Flow (5th-Percentile Currents)	Maximum Operational Flow (95th-Percentile Currents)
Intake Flow Rate (m^3/s)	0.077		0.386	
Angle to Bank (°)	360			
Mean Depth (m)	26.5			
Ambient Mean Velocity (m/s)	0.02	0.34	0.02	0.34

3.3 OSS Effluent Discharge Modeling

A total of 24 discharge scenarios were modeled with CORMIX at the large OSS to capture variability in seasons, ambient current speeds, and flow rate (Table 3-4). The effluent properties for cooling water discharged from the large OSS were determined based on the depth of the release location. All scenarios were modeled assuming a downward pointing release at a depth of 12 m. For each season the temperature and salinity profiles were used to estimate density, thus capturing potential stratification in the water column and its influence on plume dynamics. Two design flow rates were considered, 5,880,000 gallons per day (gpd) and 8,820,000 gpd, the lower bound from the 1400 MW HVDC and the upper bound from 2100 MW HVDC.

The CORMIX modeling domain was set up to reflect the site characteristics and the appropriate discharge and environmental conditions for each of the three scenarios. The ambient density of the receiving water was considered to be linearly stratified (i.e., ambient density varies linearly with depth) and was defined as such in the model by using ambient density at the surface and seabed. For each season and flow rate, simulations were performed using the 5th-, 50th-, and 95th-percentile ambient current speeds at the release depth.

Table 3-4: Summary of the input parameters used in CORMIX model simulations.

Flow Condition Description	Cooling Water Spring			Cooling Water Summer			Cooling Water Fall			Cooling Water Winter		
Discharge Location	Large OSS			Large OSS			Large OSS			Large OSS		
Ambient Current Velocity (cm/s)	5th	50th	95th	5th	50th	95th	5th	50th	95th	5th	50th	95th
	0.02	0.08	0.29	0.02	0.08	0.29	0.02	0.08	0.29	0.02	0.08	0.29
Number of Discharge Ports	1			1			1			1		
Total Flow (gpd)	1400MW	2100MW		1400MW	2100MW		1400MW	2100MW		1400MW	2100MW	
	5,880,000	8,820,000		5,880,000	8,820,000		5,880,000	8,820,000		5,880,000	8,820,000	
Discharge Flow Temperature (°C)	16.7			26.03			25.87			16.63		
Discharge Flow Density (kg/m^3)	1023.17			1020.18			1020.48			1023.62		
Pipe Orientation	Pointing Downward											
Discharge Depth (m)	12											
Pipe Diameter (in)	29.25											

The OSS effluent discharge modeling results were evaluated based on water quality standards (WQS) for temperature and residual chlorine. For the temperature WQS, the internationally recognized threshold of 3°C temperature excess of the ambient water temperature within 100 m from the discharge point was applied to the modeling (World Bank, 2015). While the 3°C temperature excess value is the primary standard, RPS evaluated each discharge scenario at a 1°C temperature excess threshold as well. The residual chlorine WQS was based on IMO, 2012 and was set to 0.5 mg/L within 100 m of the discharge point.

4 MODEL RESULTS

4.1 HZI Intake Calculations

As discussed in section 2.1, quantifying the HZI is critical to understand where impingement and entrainment of biological species in the area could occur. Conceptually, the HZI defines the line between where flow is dominated by the intake flow rate and where flow is dominated by the ambient currents. This means that at distances greater than the HZI, currents speeds are greater than the flow induced by intake of seawater and probabilistically will lead to less impingement and entrainment. Using a simplified continuity approach, the HZI's were calculated using the equation listed in section 2.1 and are presented in Table 4-1. Under all conditions, the maximum HZI is predicted to be 0.116 m from the intake location and the minimum HZI is predicted to be 0.001 m from the intake location. It should be noted that with evolving current speeds and operational intake rates, the HZI will change at the large OSS location. As the intake velocities increase and the ambient current speeds decrease, a larger HZI will form. Conversely, with higher current speeds and lower intake velocities, the HZI will decrease in size.

Table 4-1: Computed results for the HZI for each scenario.

HZI	Minimum Operational Flow (5th-Percentile Currents)	Minimum Operational Flow (95th-Percentile Currents)	Maximum Operational Flow (5th-Percentile Currents)	Maximum Operational Flow (95th-Percentile Currents)
R_{HZI} (m)	0.023	0.001	0.116	0.007
R_{HZI} (ft)	0.076	0.004	0.381	0.022

4.2 OSS Effluent Discharge Modeling

The CORMIX model was used to simulate four representative OSS effluent discharge scenarios (Table 3-4). The modeling predicted how the discharged effluent would entrain ambient water into the discharge plume, resulting in dilution. Results from this modeling study predicted the characteristics of the thermal plume (i.e., magnitude and extent) as described by the location, size (i.e., radius, width, height), and associated dilution. Dilution was reported at 100 m from the discharge location along the plume centerline. The center of the plume contains the highest anticipated concentrations, with concentrations diminishing away from the centerline.

A succinct summary of the model results includes: (1) downstream distance to the WQS of 3°C excess, (2) the downstream distance to the WQS of 0.5 mg/L chlorine residual , (3) the dilution factor at 100 m downstream distance, and (4) the lateral plume radius at 100 m downstream distance (Table 4-2). The predicted effluent plume characteristics varied for each scenario with dilution factors, distances, and time varying by several orders of magnitude. To standardize results for comparison with one another, the plume centerline dilution factor and the maximum plume extent (i.e., radius or thickness) were provided at a location 100 m from the discharge.

Table 4-2: Summary of plume dilution and extent.

Season	Water Quality Standard: 3°C Excess Downstream Distance (m)	Water Quality Standard: 0.5 mg/L Chlorine Residual Downstream Distance (m)	Dilution Factor at 100 m Distance	Lateral Plume Radius (m) at 100 m Distance
1400 MW Cooling Water Discharge				
Spring 5th percentile	1.39	0.29	49.1	191.19
Spring 50th percentile	4.75	0.60	38.3	33.00
Spring 95th percentile	7.68	0.38	52.8	8.32
Summer 5th percentile	0.96	0.38	20.8	137.62
Summer 50th percentile	3.68	0.61	15.2	32.22
Summer 95th percentile	6.58	0.40	33.2	12.75
Fall 5th percentile	0.84	0.38	80.7	296.46
Fall 50th percentile	3.61	0.60	39.0	40.34
Fall 95th percentile	6.46	0.38	64.3	10.39
Winter 5th percentile	1.23	0.29	55.1	210.81
Winter 50th percentile	4.49	0.59	48.1	34.78
Winter 95th percentile	7.54	0.38	67.6	8.48
2100 MW Cooling Water Discharge				
Spring 5th percentile	1.64	0.12	55.2	264.43
Spring 50th percentile	4.99	0.42	34.2	37.68
Spring 95th percentile	3.63	0.43	49.2	9.42
Summer 5th percentile	1.04	0.17	17.3	158.32
Summer 50th percentile	15.69	5.38	7.1	44.68
Summer 95th percentile	31.94	5.80	7.1	12.76
Fall 5th percentile	1.04	0.18	64.8	379.13
Fall 50th percentile	4.29	0.53	32.6	46.55
Fall 95th percentile	7.05	0.43	57.8	11.74
Winter 5th percentile	1.51	0.13	58.8	291.60
Winter 50th percentile	4.98	0.42	41.6	39.63
Winter 95th percentile	3.81	0.43	61.4	9.58

In addition to the summary metrics presented in Table 4-2 detailed results for each season were developed and presented as a series of plots depicting the location of the plume's centerline within the water column, temperature excess, chlorine residual concentration, and lateral extents with respect to distance from the outfall under each current condition (5th, 50th-, 95th- percentile) and flow rate.

The discussions provided for each scenario describe the range of predicted results and reiterate the metrics summarized in Table 4-2. Metrics of temperature excess and chlorine residual were computed based upon the dilution factor of the models. The dilution factor is a ratio of the initial concentration to concentration at the given location. The WQS for temperature excess of 3°C and chlorine residual of 0.5 mg/L are included in the relevant plots as a dashed line.

4.2.1 Spring

For both the 1400 MW and 2100 MW release scenarios, the plume associated with the 5th-percentile current speed was predicted to extend the deepest, followed by the 50th-percentile simulation, and the shallowest plume was associated with the 95th-percentile conditions (Figure 4-1). This occurs because the subsurface currents deflect the plume in the direction of flow and happens more readily for the higher magnitude speeds because of its relative influence compared to the downward momentum induced from the discharge pipe. The influence of flow rate is also readily observed by these results, with the higher flow rate (2100 MW HVDC) causing the plumes to extend deeper into the water column compared with the 1400 MW HVDC for all current conditions. Once the jet reaches its maximum depth, the influence of the currents and its impact on dilution is clear as the buoyant thermal plume rises towards the water surface.

For all spring scenarios and flow rates, the thermal plume diluted sufficiently to result in excess temperatures of below 1°C and the 3°C WQS threshold regardless of current speed (Figure 4-2). The downstream distances associated with this 3°C excess WQS varied by current speed, with the slowest current speed scenario predicted to dilute below this 3°C excess standard closer to the release point than the 50^{th-} and 95th-percentile current conditions (Table 4-2) for the 1400 MW and 2100 MW HVDC scenarios. This occurred because of the initial downward forcing which induced mixing due to momentum and rapid dilution due to density gradients in the water column.

The WQS of 0.5 mg/L for residual chlorine was predicted to be met for all spring simulations regardless of flow rate or current speed (Figure 4-3). Unlike the thermal plume dilution, the 1400 MW HVDC flow rate for the 50th-percentile was estimated to reach the residual chlorine threshold slightly further from the source than for the 95th-percentile currents. This inflection can also be noticed in the dilution factor at 100 m (Table 4-2) for the 1400 MW and 2100 MW HVDC scenarios. In these scenarios, the 50th-percentile current speeds are large enough to overcome the downward momentum of the effluent, but not significant enough to induce adequate mixing as occurred for the 95th-percentile currents simulations. The influence of current speeds on the lateral spreading was most obvious for the 5th-percentile current speeds in both the 1400 MW and 2100 MW HVDC simulations (Figure 4-4).

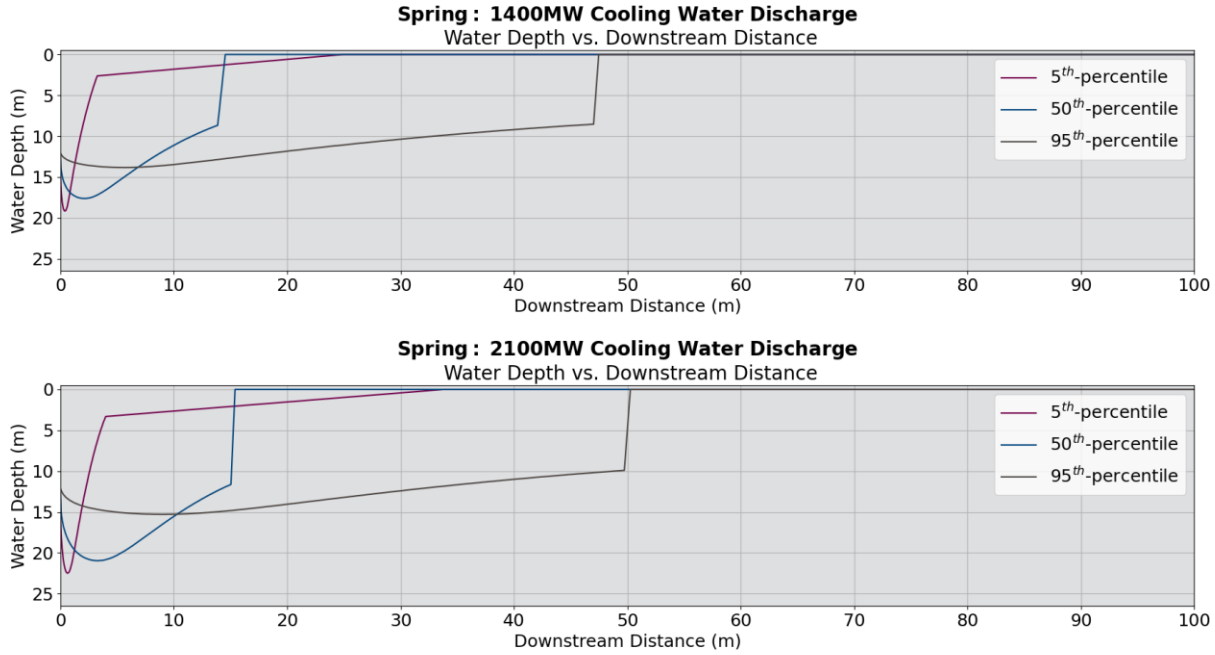

Figure 4-1: Effluent discharge water depth versus downstream distance under spring conditions.

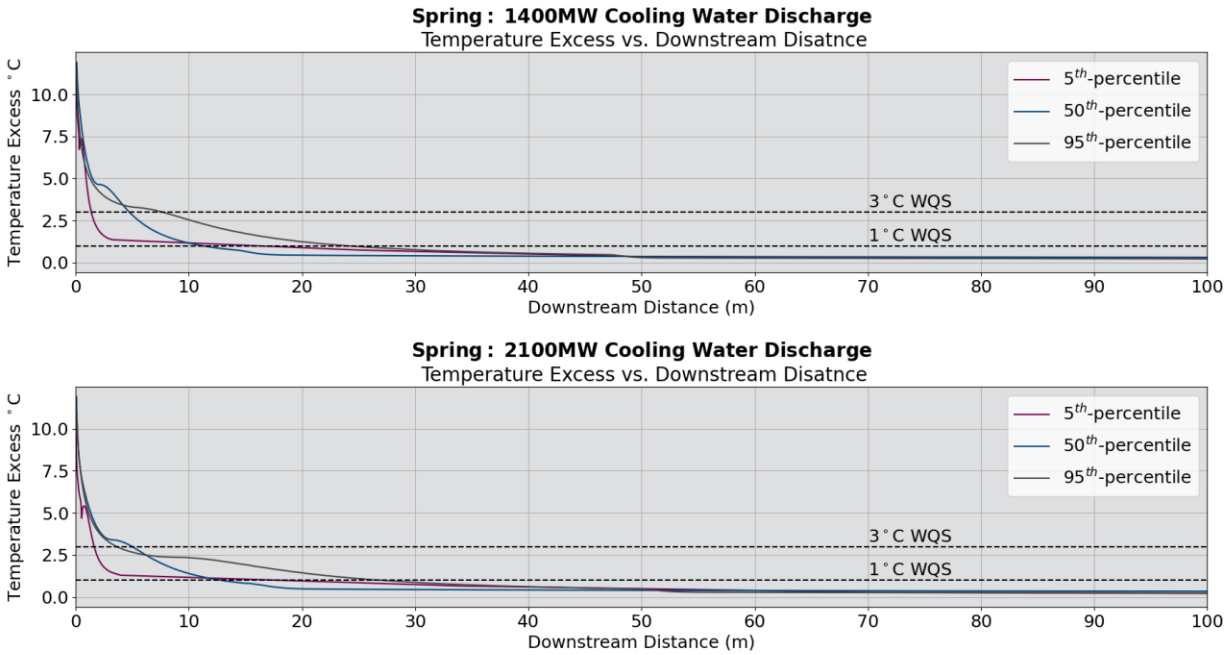

Figure 4-2. Effluent discharge temperature (°C) excess versus downstream distance under spring conditions.

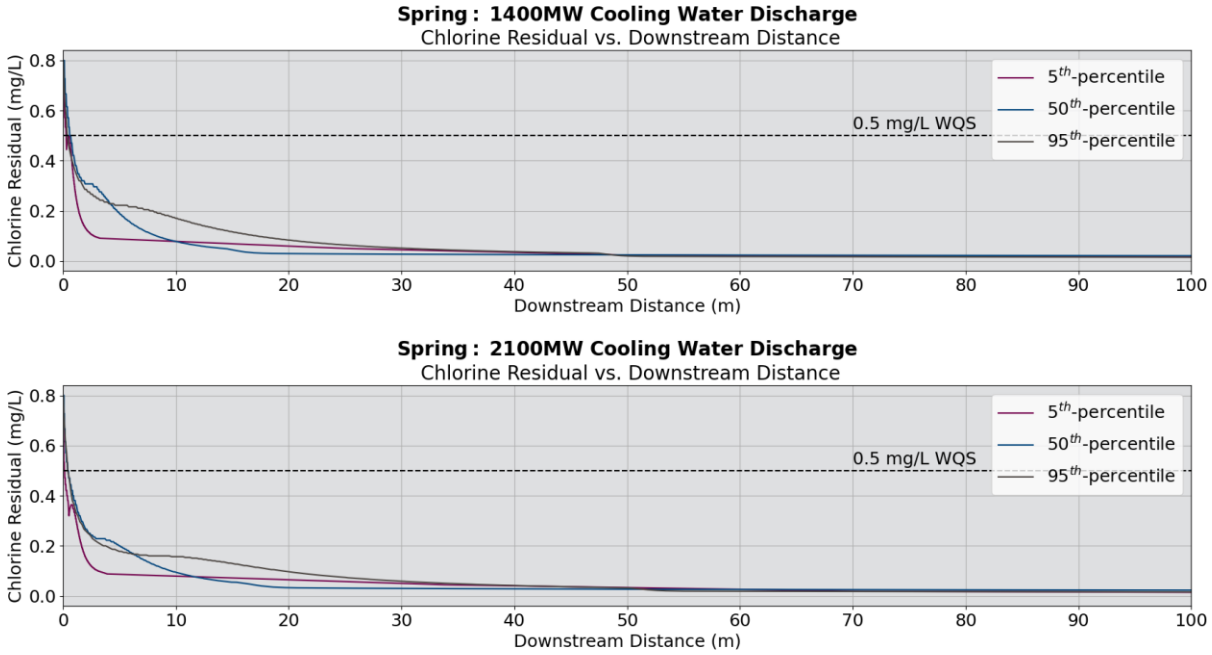

Figure 4-3. Effluent discharge residual chlorine (mg/L) versus downstream distance under spring conditions.

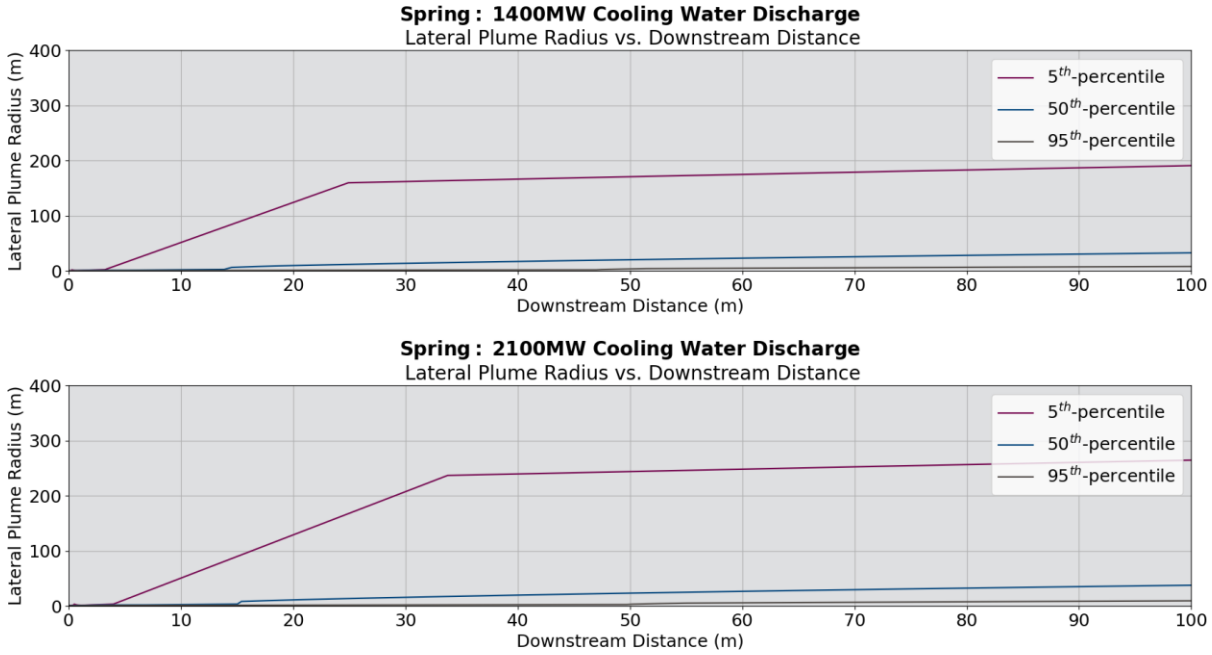

Figure 4-4: Effluent discharge lateral plume radius versus downstream distance under spring conditions.

4.2.2 Summer

Similar to the spring simulations for the 1400 MW HVDC scenarios, the vertical extent of the plume was predicted to be deeper for the 5th-percentile simulation than for the 50th- and 95th-percentile simulations (Figure 4-5). Due to the warmer ambient water temperatures, the density driven dilution was less pronounced for summer than in the spring which changed the shape of the vertical plume extent for all conditions. This was especially noticeable for the 2100 MW HVDC summer scenarios, in that the plume surfaces immediately. This occurred due to the Coanda effect, a phenomenon which occurs when the fluid attaches to the convex surface of the orifice opening and rises immediately to the surface along the discharge pipe. This minimized the potential for momentum induced mixing which ultimately reduced the dilution associated with these two simulations (2100 MW HVDC, 50th and 95th summer simulations) compared with all other scenarios (Table 4-2).

The WQS of 3°C temperature excess was predicted to be met for all summer scenarios, including all flow rates and current conditions (Figure 4-6). However, the 1°C temperature excess value was not met for the 50th- and 95th-percentile 2100 MW HVDC discharge scenarios, which is due to the Coanda effect mentioned previously. The WQS of 0.5 mg/L for residual chlorine was estimated to fall below the threshold for all summer scenarios, flow rates, and current conditions as well (Figure 4-7). The 2100 MW HVDC simulations for the 50th- and 95th-percentile current speeds resulted in the WQS for residual chlorine being met further from the discharge pipe than the 1400 MW cooling water discharge condition. This again was due to the Coanda effect, which inhibited mixing near the discharge point (Table 4-2).

As with the spring simulations, the lateral plume radius extends further horizontally under lower current speeds in summer for both 1400 MW and 2100 MW HVDC release conditions (Figure 4-8). This can be attributed to the greater influence of lateral dispersion rather than advection-induced transport due to ambient currents. The released plumes are able to spread within the water column while the slow-moving currents carry the plume downstream. Conversely, with higher current speeds, the momentum from advection-induced transport inhibits spreading while the plume continues downstream from the release location (Table 4-2)

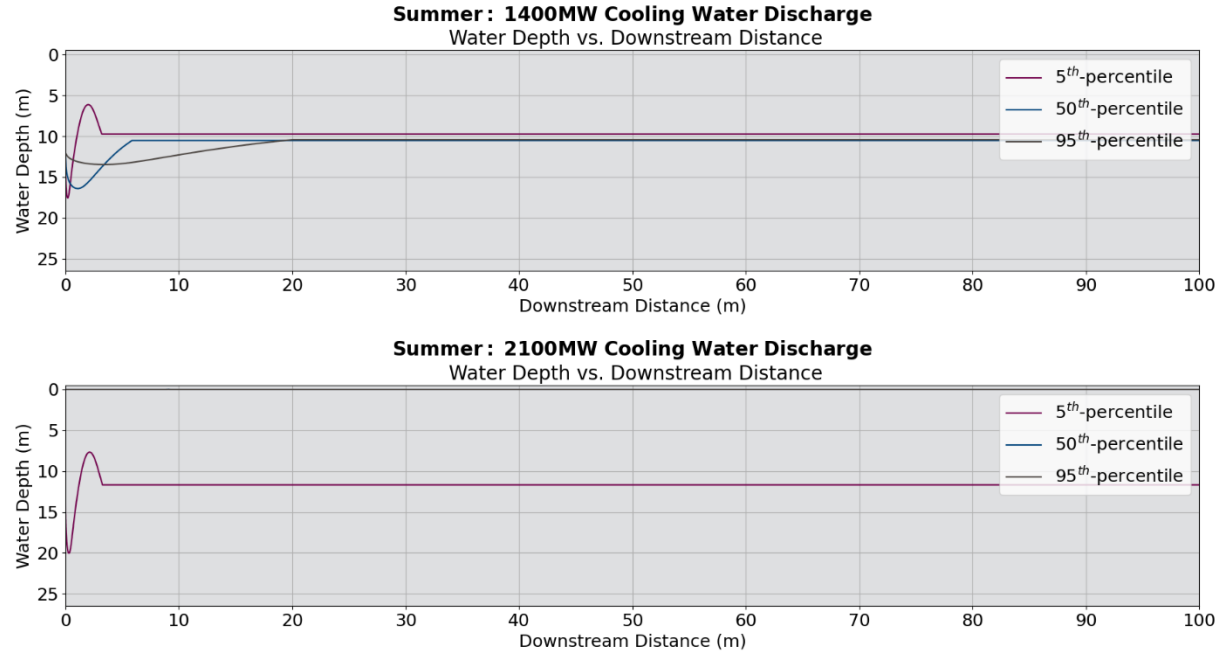

Figure 4-5: Effluent discharge water depth versus downstream distance under summer conditions.

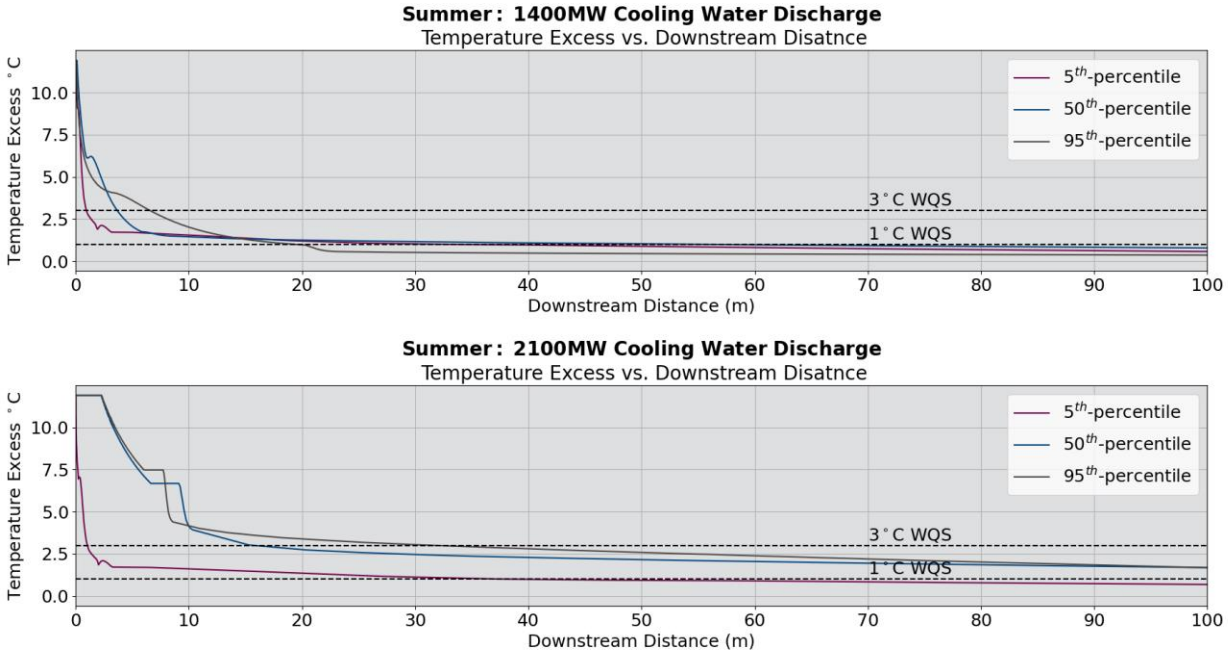

Figure 4-6: Effluent discharge temperature (°C) excess versus downstream distance under summer conditions.

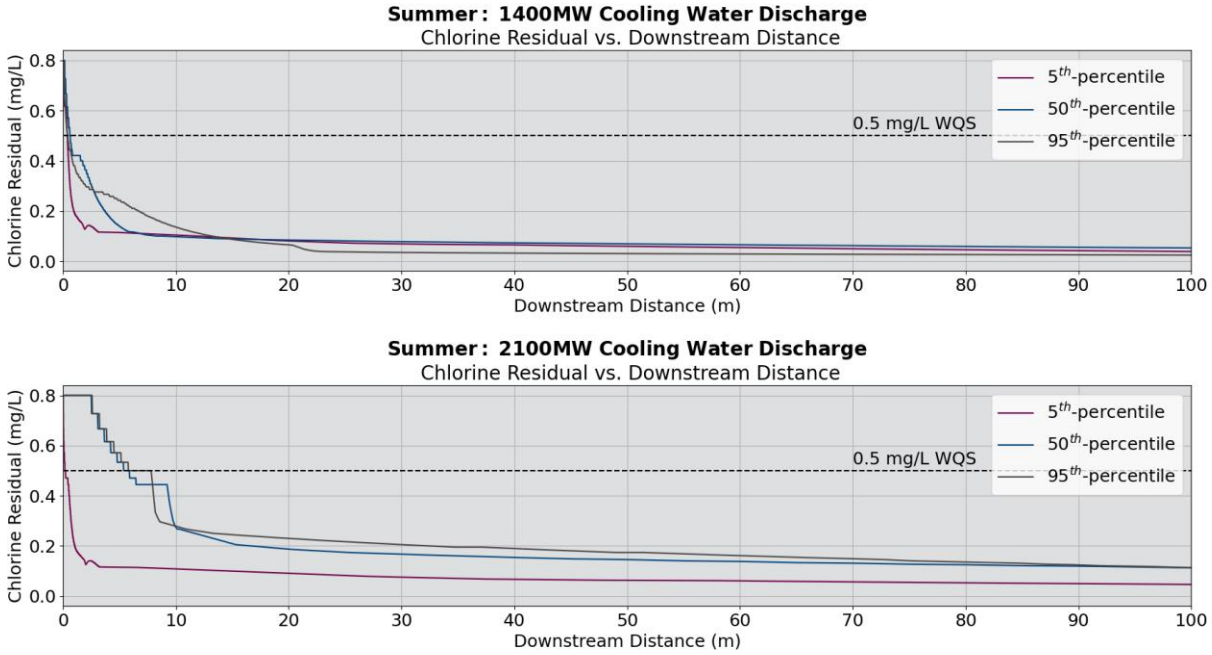

Figure 4-7. Effluent discharge residual chlorine (mg/L) versus downstream distance under summer conditions.

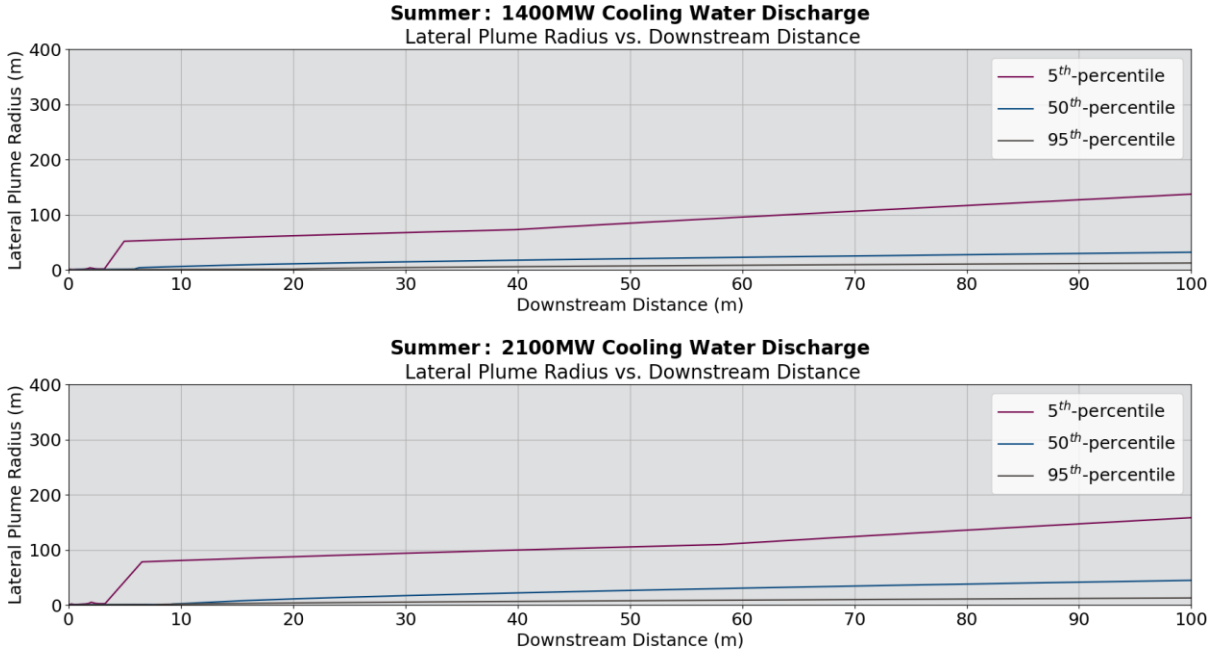

Figure 4-8: Effluent discharge lateral plume radius versus downstream distance under summer conditions.

4.2.3 Fall

Like the spring simulations for the 1400 MW and 2100 MW scenarios, the vertical extent of the plume was predicted to be deeper for the 5th-percentile simulation than for the 50th- and 95th-percentile simulations during the fall scenarios (Figure 4-9). As previously stated, subsurface currents deflect the plume as it is discharged into the water column, where more deflection coincides with higher magnitude speeds in the

direction of flow. The influence of flow rate is also readily observed by these results, with the higher flow rate scenarios (2100 MW HVDC) predicting the discharged plumes to extend deeper into the water column compared to the 1400 MW HVDC for all current conditions.

The WQS of 3°C temperature excess, as well as the evaluated 1°C temperature excess value, was predicted to be met within 10 m of the discharge point for all fall discharge scenarios (Figure 4-10). Similarly, the WQS of 0.5 mg/L for residual chlorine concentration was predicted to be met for all fall simulations regardless of flow rate or current speed (Figure 4-11). When comparing the distances that the residual chlorine concentration thresholds are met, the 2100 MW HVDC scenarios generally dilute the effluent closer to the discharge point than for the 1400MW HVDC scenarios. This can be attributed to the larger rate of discharge from the 2100 MW HVDC, which initially promotes greater initial momentum-induced mixing (Table 4-2).

The trend of increasing lateral plume radii for decreasing current speeds observed during the summer and spring scenarios is also predicted for the fall scenarios (Figure 4-12). For both the 1400 MW and 2100 MW HVDC scenarios, the 5th-percentile current speed cases exhibited larger lateral plume radii when compared to the higher magnitude 50th- and 95th-percentile current speeds. As stated above, this is due to the greater influence of lateral dispersion rather than advection-induced transport due to ambient currents (Table 4-2).

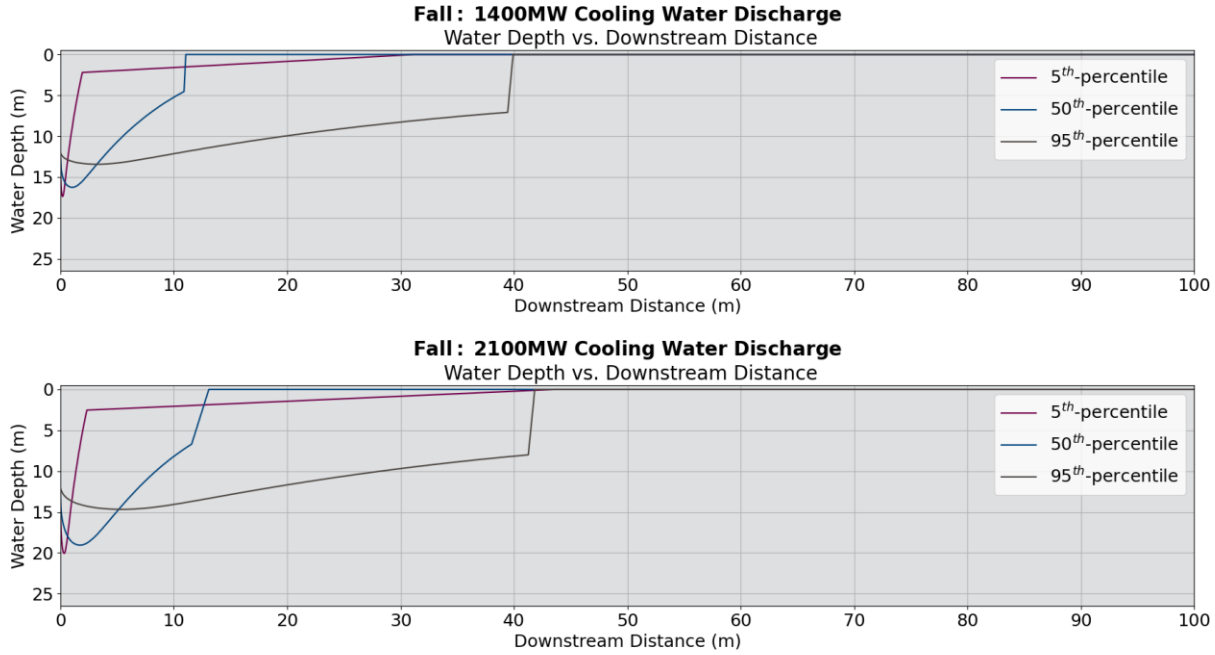

Figure 4-9. Effluent discharge water depth versus downstream distance under fall conditions

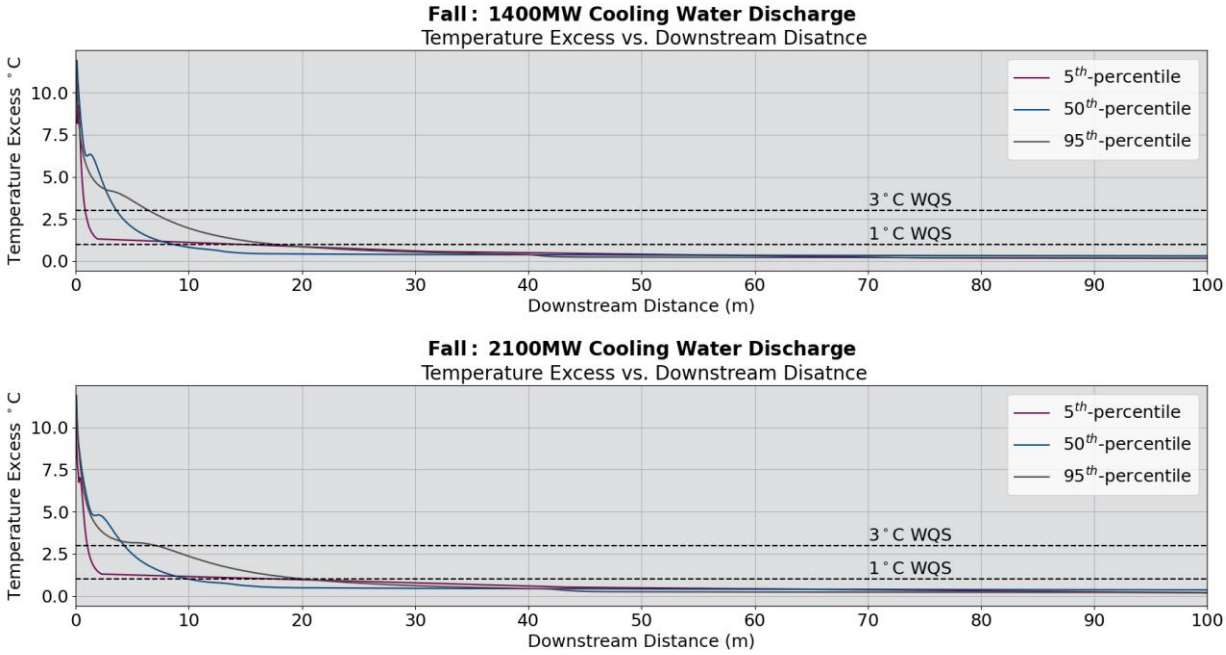

Figure 4-10. Effluent discharge temperature (°C) excess versus downstream distance under fall conditions.

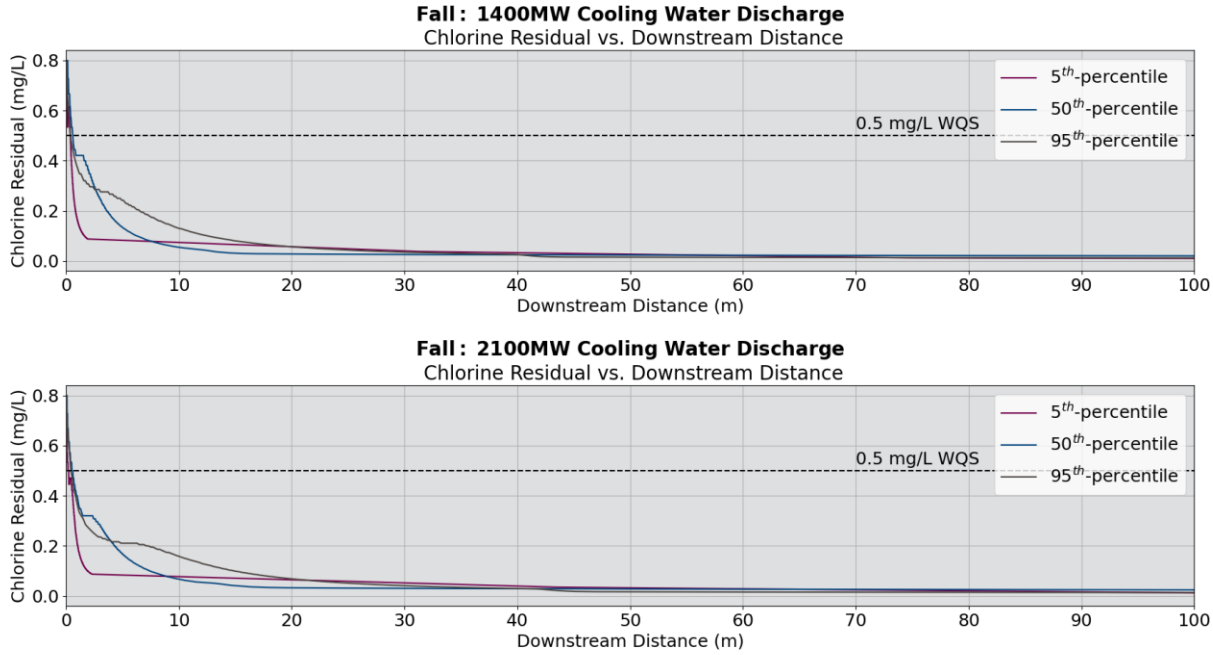

Figure 4-11. Effluent discharge residual chlorine (mg/L) versus downstream distance under fall conditions.

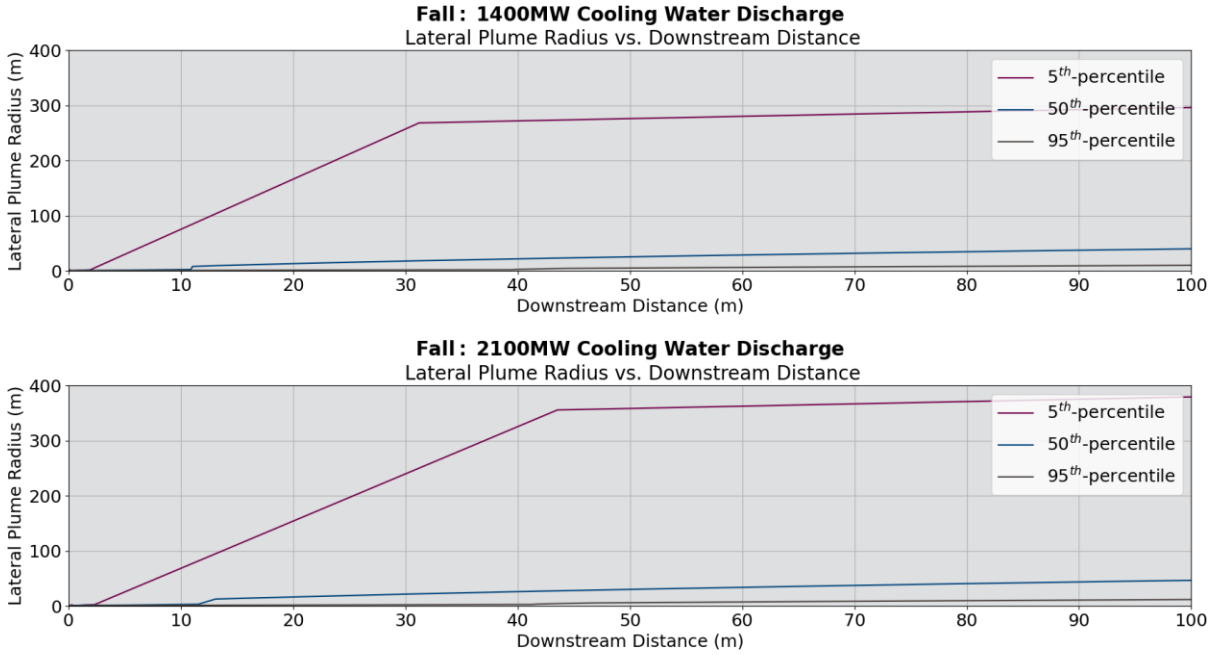

Figure 4-12. Effluent discharge lateral plume radius versus downstream distance under fall conditions.

4.2.4 Winter

All winter simulations displayed similar results compared to the fall and spring simulations regarding the predicted vertical extents of the discharged plumes (Figure 4-13). The 5th-percentile current speed scenarios for both the 1400 MW and 2100 MW HVDC's were predicted to reach greater depths than compared to the 50th- and 95th-percentile current speed scenarios. The 2100 MW HVDC scenarios remained within the water column at further downstream distances than the 1400 MW HVDC scenarios. This is due to the larger discharge flow rate simulated for the 2100 MW HVDC, which allows the effluent plume to reach greater depths than compared to the 1400 MW HVDC cases.

The WQS' of 3°C temperature excess and 0.5 mg/L residual chlorine were predicted to be met within 10 m of the discharge point for all winter scenarios (Figure 4-14 and Figure 4-15). Similarly, the evaluated 1°C temperature excess value was also met within 30 m of the discharge point (Figure 4-14). This is due to the relatively homogenous density profile within the water column which allowed the thermal plume to sufficiently mix through momentum-induced and buoyancy-induced mixing after it had been discharged into the environment. Because of this, the winter simulations for both the 1400 MW and 2100 MW HVDC's exhibited increased mixing for the 50th- and 95th-percentile current speeds compared to all other seasons (Table 4-2). As observed for all previously evaluated seasons, the winter simulations also exhibited decreasing lateral plume radius predictions with increasing current speeds for both the 1400 MW and 2100 MW HVDC cases (Figure 4-16). Higher current speeds inhibit spreading of the plume as it travels downstream, leading to smaller lateral plume radius extents at the 100 m distance (Table 4-2).

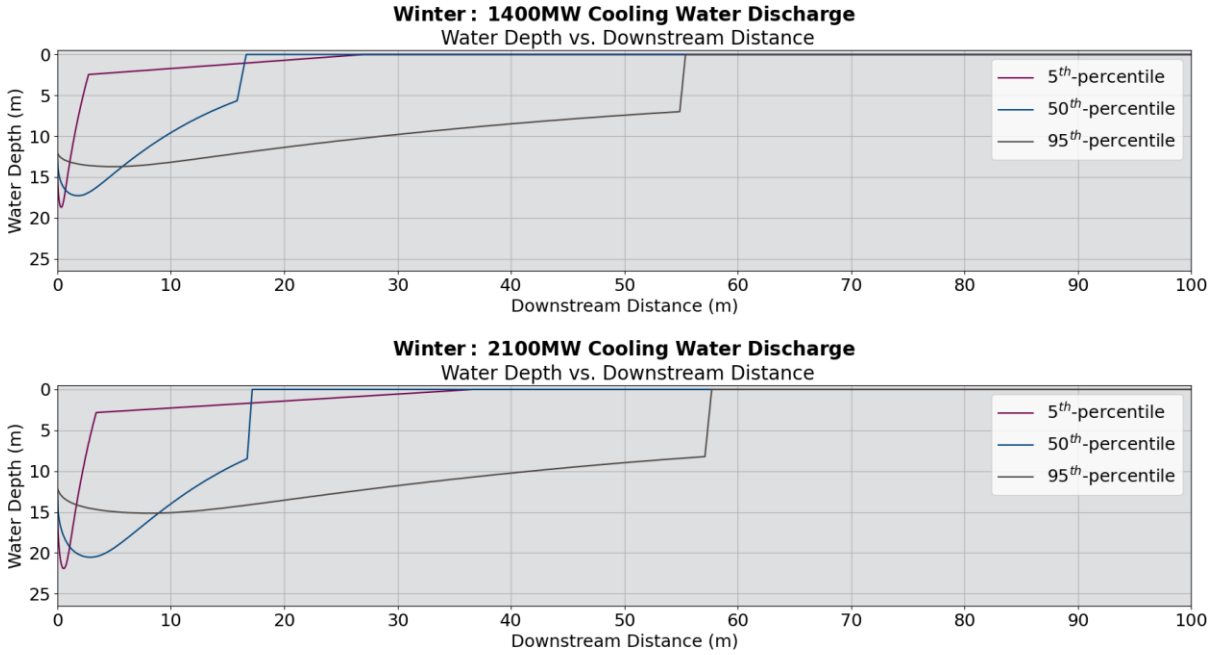

Figure 4-13. Effluent discharge water depth versus downstream distance under winter conditions.

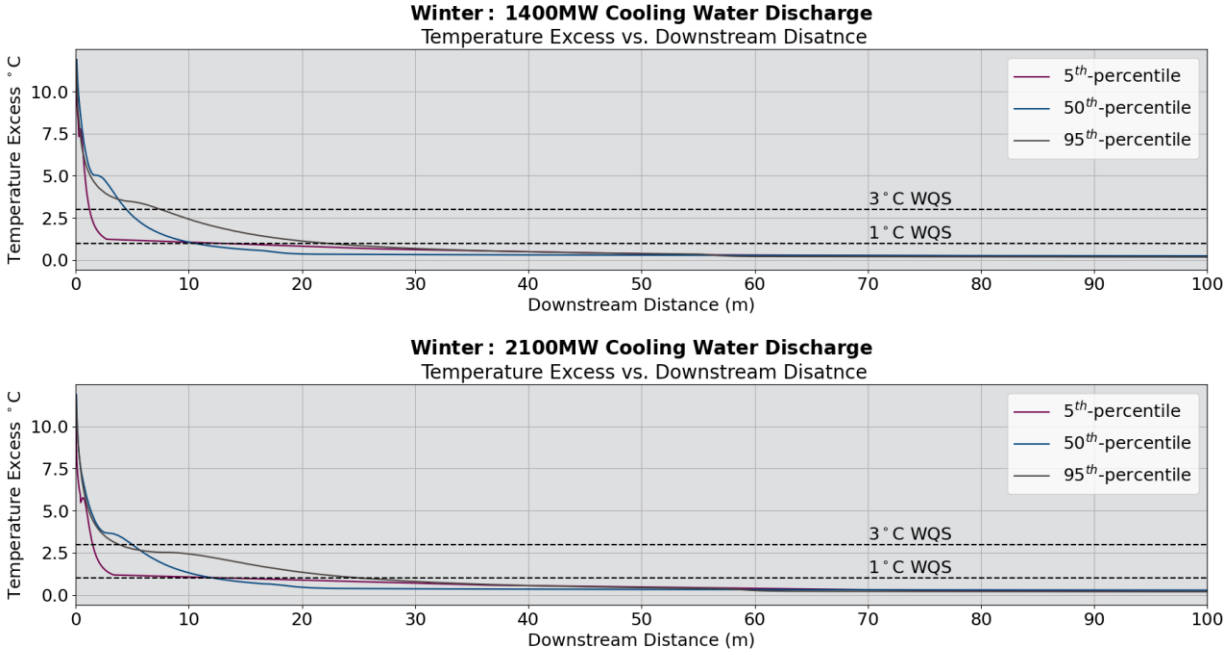

Figure 4-14. Effluent discharge temperature (°C) excess versus downstream distance under winter conditions.

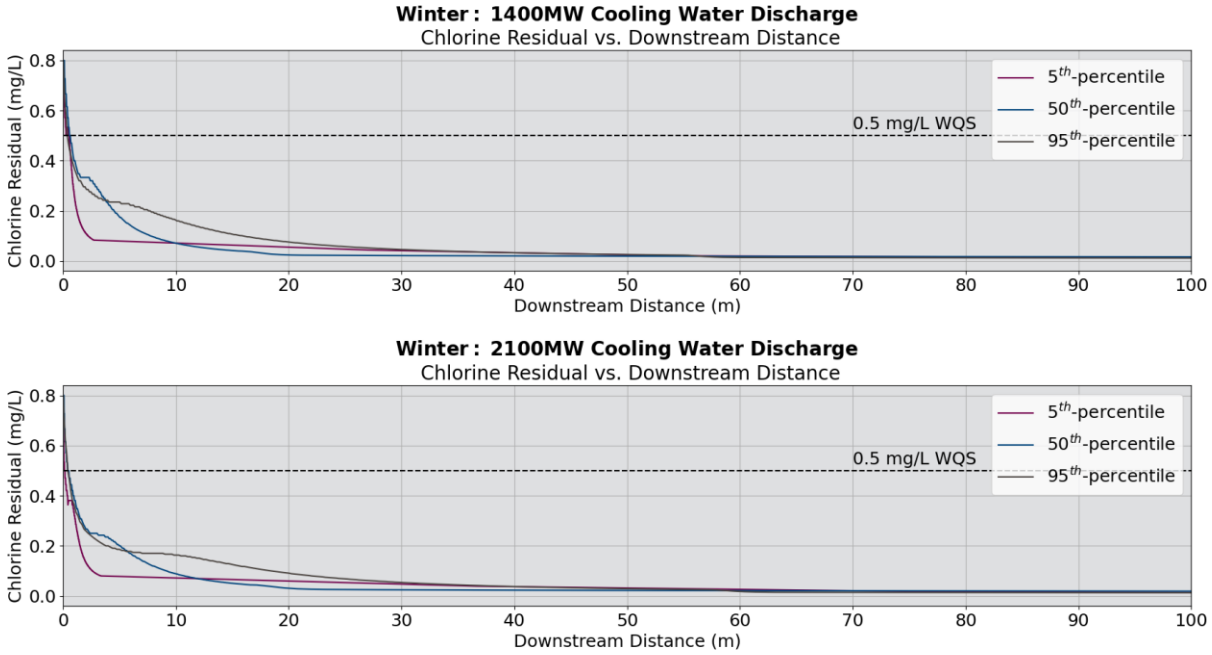

Figure 4-15. Effluent discharge residual chlorine (mg/L) versus downstream distance under winter conditions.

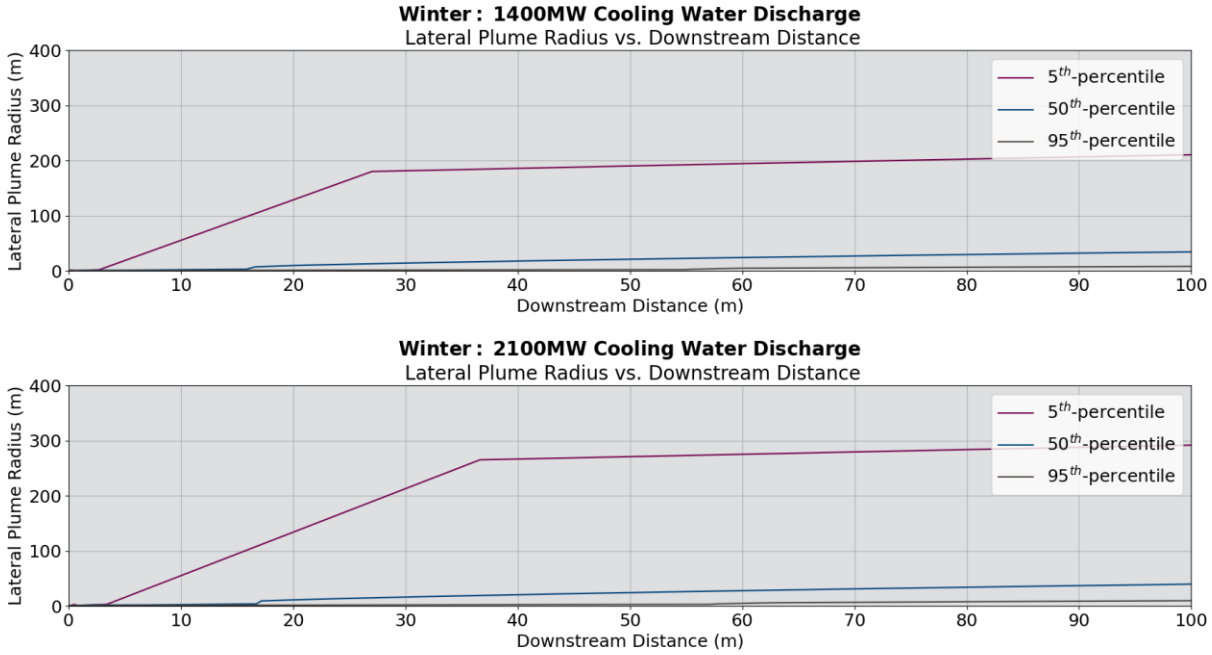

Figure 4-16. Effluent discharge lateral plume radius versus downstream distance under winter conditions.

5 DISCUSSION AND CONCLUSION

5.1 Large OSS HZI and Effluent Discharges Discussion

This study was conducted to assess the HZI's formed during operational intake of seawater and hypothetical effluent plumes spanning the range of anticipated discharges associated with the Atlantic Shores large OSS Project site. For the HZI calculations, 4 scenarios were evaluated using a simplified approach to bound the upper and lower limits of the HZI's that will form during operations. The study also included 24 discharge scenarios that accounted for seasonality, evolving current speeds, and two separate discharge rates for cooling water discharge. Effluent discharge scenarios were simulated using CORMIX, a USEPA-approved dilution and mixing zone modeling system. The simulations were performed assuming steady-state releases of a conservative (i.e., non-reacting, non-settling, non-decaying) constituent and assuming several different environmental forcing conditions. The results provided in this assessment are therefore useful in determining the scale and magnitude of potential effects. However, note that considerations may be required when reviewing results in the context of or for comparative purposes with one another and with respect to any specific release at a point in time.

The calculations for the HZI are highly dependent on the ratio between the ambient current velocity and the intake rate. Results showed that with larger intake rates and lower current velocities, predicted HZI values are expected. For the large OSS intake systems, a maximum HZI value of 0.116 m is predicted, which coincides with the largest expected operational intake rate and the 5th percentile ambient current speeds. Conversely, the lowest HZI value of 0.001 m is predicted with the lowest expected operational intake rate and the 95th percentile ambient current speeds. During operations at the large OSS, the HZI will vary with changing current speeds and intake rates, so consideration of these changes should be taken into account when evaluating the potential impingement and entrainment of local species.

The effluent discharges simulations predicted that through all scenarios (i.e., all current speeds, seasons, and discharge rates), the discharged cooling water experienced rapid mixing upon release and dropped below the 3°C temperature excess and 0.5 mg/L residual chlorine concentration WQS' within 100 m of the discharge point. For majority of the simulations, these thresholds were met within 10 m of the discharge point. Two scenarios (2100 MW HVDC Summer 50th- and 95th-percentile current speed scenarios) resulted in the plume reaching up to 32 m before the thresholds were met. This is a product of the Coanda effect (Doneker and Jirka, 2001), where the effluent streams are predicted to attach to the discharge pipe and sea surface, which leads to less momentum-induced mixing. However, these two scenarios still sufficiently mix with the ambient water and are predicted to be less than 2°C in temperature excess and less than 0.2 mg/L of residual chlorine concentration by 100 m away from the discharge port (Table 4-2).

When evaluating the effects seasonality had on the effluent discharge results, there is a distinct difference between the four seasons. For both the 1400 and 2100 MW HVDC's, the effluent is predicted to dilute the least during the summer seasons, where a dilution factor of 15.2 (0.8°C excess and 0.05 mg/L of residual chlorine) and 7.1 (1.7°C excess and 0.11 mg/L of residual chlorine) is expected 100 m away from the discharge port. This is likely due to the increased stratification of the water during the summer, which can prohibit buoyancy-induced mixing of the effluent. Contrarily, the effluent is predicted to dilute the most during the winter seasons scenarios for both the 1400 and 2100 MW HVDC discharge rates. The relatively homogenous stratification during this season allows effluent plume to mix with the ambient water as it travels downward from the discharge port, as well as up towards the surface through buoyancy effects (Table 4-2).

Current speeds also affect the mixing potential of the discharged cooling water. In general, the simulated effluents fall below the thresholds of concern closest to the discharge point during the 5th-percentile current cases. During these scenarios, the discharged effluent can travel a further distance down into the water

column where it continues to mix before the current-induced advection moves the plume downstream. The 95th-percentile current speed scenarios travel the greatest distance downstream before falling below the thresholds of concern. The currents transport the plumes laterally, causing them to dilute less in the near-field. However, the induced mixing from the higher speed currents generally enhance mixing in the far-field (Table 4-2).

5.2 Model Considerations and Conclusions

The HZI calculations predicted that the hydraulic influence due to intake of ambient seawater would be confined within less than 0.2 m from the intake point for all scenarios calculated. For all simulated effluent discharges cases, the WQS' for both temperature and residual chlorine met the regulatory limit within the defined mixing zone of 100 m from the discharge point. HZI and plume predictions were influenced by the set of underlying assumptions used in the calculations and modeling. This study provides general findings based upon conditions from multiple years of data and steady state currents. However, the magnitude and direction of currents and the actual environmental conditions in receiving waters are dynamic (on time scales <1 min and on spatial scales <1 m), which would impact the characteristics and timing of the HZI formation and discharged effluent plumes. Therefore, the predicted spatial results associated with HZI formation and longer plume development times (e.g., tens of minutes or hours) may be affected by changing environmental conditions.

While there may be some associated caveats in the predicted HZI and dilution trends of each of the simulated scenarios, the presented HZI equation and CORMIX model were used to effectively simulate representative intake and discharge scenarios that are expected at the large OSS. The modeling captured the types of gradients (e.g., T, S, density) and broad range of magnitudes (volume and rate) of effluent discharge that are expected, as well as the variable environmental and operational conditions that the HVDC intake systems would experience. Therefore, even with the considerations noted previously in this section, HZI predictions and computational effluent discharge modeling was effectively used to predict the range of magnitudes, and extents of both the HZI and effluent plume dilution within the ambient environment.

6 REFERENCES

Beardsley, R.C. and Winant, C.D., 1979. On the mean circulation in the Mid-Atlantic Bight. *Journal of Physical Oceanography*, *9*(3), pp.612-619.

Conkright, M.E., Locarnini, R.A., Garcia, H.E., O'Brien, T.D., Boyer, T.P., Stephens, C. and Antonov, J.I., 2002. World Ocean Atlas 2001: Objective analyses, data statistics, and figures: CD-ROM documentation.

Cummings, J.A., 2005. Operational multivariate ocean data assimilation. Quarterly Journal of the Royal Meteorological Society, 131(613), pp.3583-3604.

Cummings, J.A. and Smedstad, O.M., 2013. Variational data assimilation for the global ocean. In Data Assimilation for Atmospheric, Oceanic and Hydrologic Applications (Vol. II) (pp. 303-343). Springer, Berlin, Heidelberg.

Doneker, R.L. and G.H. Jirka, CORMIX User Manual: A Hydrodynamic Mixing Zone Model and Decision Support System for Pollutant Discharges into Surface Waters, EPA-823-K-07-001, Dec. 2007.

Doneker RL, Jirka GH. CORMIX-GI systems for mixing zone analysis of brine wastewater disposal. Desalination. 2001 Sep 20;139 (1-3):263-74.

Doneker, R.L. and G.H. Jirka, "Expert Systems for Hydrodynamic Mixing Zone Analysis of Conventional and Toxic Single Port Discharges (CORMIX1)", Technical Report EPA/600/3-90/012, U.S. EPA Environmental Research Laboratory, Athens, GA 1990.

Fox, D.N., Teague, W.J., Barron, C.N., Carnes, M.R. and Lee, C.M., 2002. The modular ocean data assimilation system (MODAS). Journal of Atmospheric and Oceanic Technology, 19(2), pp.240-252.

Golder Associates Inc., 2008. Source water and cooling water data and impingement mortality and entrainment characterization for Monroe power plant. July 2008. Prepared for Detroit Edison Company. Project 063-9564. 444 pp. Gong, D., Kohut, J.T. and Glenn, S.M., 2010. Seasonal climatology of wind-driven circulation on the New Jersey Shelf. Journal of Geophysical Research: Oceans, 115(C4).

Halliwell, G.R., 2004. Evaluation of vertical coordinate and vertical mixing algorithms in the HYbrid-Coordinate Ocean Model (HYCOM). Ocean Modelling, 7(3-4), pp.285-322.

International Maritime Organization (IMO), 2012. Guidelines on Implementation of Effluent Standards and Performance Tests for Sewage Treatment Plants. Resolution MEPC.22764. Adopted on 5 October 2012.

Kohut, J.T., Glenn, S.M. and Chant, R.J., 2004. Seasonal current variability on the New Jersey inner shelf. Journal of Geophysical Research: Oceans, 109(C7).

Levitus, S., 1982. Climatological atlas of the world ocean. NOAA Profess. Pap., 13, pp.1-173.

Levitus S., Boyer, T.P., Garcia, H.E., Locarnini, R.A., and Zweng, M.M. 2014. World ocean atlas 2013 (NODC accession 0114815). Silver Spring (MD): NOAA.

Locarnini, R. A., Mishonov, A. V., Baranova, O. K., Boyer, T. P., Zweng, M. M., Garcia, H. E., Reagan, J. R., Seidov, D., Weathers, K., Paver, C. R., and Smolyar, I. 2018. World Ocean Atlas 2018, Volume 1: Temperature. A. Mishonov Technical Ed.; NOAA Atlas NESDIS 81, p.52.

Richardson, J. and Dixon, D., 2004. Modeling the Hydraulic Zone of Influence of Connecticut Yankee Nuclear Power Plant's Cooling Water Intake Structure. American Fisheries Society, Monograph 9.

Richaud, B., Kwon, Y.O., Joyce, T.M., Fratantoni, P.S. and Lentz, S.J., 2016. Surface and bottom temperature and salinity climatology along the continental shelf off the Canadian and US East Coasts. Continental Shelf Research, 124, pp.165-181.

Saha, S., Moorthi, S., Pan, H.L., Wu, X., Wang, J., Nadiga, S., Tripp, P., Kistler, R., Woollen, J., Behringer, D. and Liu, H., 2010. The NCEP climate forecast system reanalysis. Bulletin of the American Meteorological Society, 91(8), pp.1015-1058.

Wiegel, R.L., 1964. Oceanographic Engineering, Prentice-Hall, Inc, Englewood Cliffs, N.J.

World Bank, 2015. Environmental, health, and safety guidelines for offshore oil and gas development English. IFC E&S. Washington, D.C.: World Bank Group. Available at: https://documents1.worldbank.org/curated/en/378221479466912449/pdf/110348-FINALJun-2015-Offshore-Oil-and-Gas-EHS-Guideline-PUBLIC.pdf.

Zweng, M. M., Reagan, J. R., Seidov, D., Boyer, T. P., Locarnini, R. A., Garcia, H. E., Mishonov, A. V., Baranova, O. K., Weathers, K., Paver, C. R., and Smolyar, I., 2018. World Ocean Atlas 2018, Volume 2: Salinity. A. Mishonov Technical Ed.; NOAA Atlas NESDIS 82, p.50.